www.editada.org

International Journal of Combinatorial Optimization Problems and Informatics, 17(4), 2026, 180-204. ISSN: 2007-1558.
https://doi.org/10.61467/2007.1558.2026.v17i4.1317

Unveiling Structural Dynamics in Supply Chains' Resilience: A Multi-Effects High-Frequency Panel Analysis

Fabricio Moreno-Baca[1,2], Tomas Veloz[3], Patricia Cano-Olivos[1],
Diana Sánchez-Partida[1], José-Luis Martínez-Flores[1]

[1] Department of Logistics and Supply Chain Management, Universidad Popular Autónoma del Estado de Puebla (UPAEP), México. [2] Center Leo Apostel, Vrije Universiteit Brussel, Belgium. [3] Departamento de Matemáticas, Universidad Tecnológica Metropolitana, Santiago 833038, Chile.

Email address(es): fabricio.moreno@upaep.edu.mx, tomas.veloz@vub.be, patricia.cano@upaep.mx, diana.sanchez@upaep.mx, joseluis.martinez01@upaep.mx

Abstract. This study presents a novel methodology for analyzing the inherent structural behaviour of supply chain resilience (SCR) by integrating logistics multi-effects, such as Synchronization, Spillover, Bullwhip, Ripple, Economic, and strategic decision-making processes. We propose a hierarchical nonlinear state-space model, which is applied to the Mexican maritime port system (2008–2023) to analyze resilience in the context of two major disruptions: the global financial crisis (2008–2009) and the COVID-19 pandemic (2020–2023). The results show that the Bullwhip effect acts as an early-warning signal, while Spillover effects negatively affected resilience in both periods, with greater intensity during the pandemic. Synchronization was the only consistently positive effect and the primary driver of resilience, especially during health crises, by aligning information, decisions, and timing under high uncertainty. The Ripple effect was context-dependent: detrimental during economic crises due to the amplification of failures, but positive during pandemics by accelerating coordinated responses.
Keywords: Supply Chain Resilience, Hierarchical Bayesian Models, Particle Filtering, Resilience Dynamics, Panel Data, Exogenous Shocks, Structural Nonlinearity, Transfer Entropy.

Article information
Received: Jan 31, 2026
Accepted: Jun 11, 2026

1 Introduction

Resilience in a supply chain is crucial for maintaining stability and responding to unexpected events. Modern supply chains operate in complex, highly interconnected environments, where factors such as natural disasters, pandemics, cyberattacks, and economic fluctuations can disrupt the flow of goods and services (Chowdhury et al., 2021). Understanding these risks and modeling resilience allows companies to minimize losses, optimize resources, and maintain operational continuity, thereby enabling rapid recovery from disruptions (Juan et al., 2022). Figure 1 shows the resilience framework, illustrating how a system's operational level shifts before, during, and after a significant disruption. Preparation encompasses forward-looking measures and planning aimed at reducing the likelihood and impact of disruptions. These measures include robust design principles, targeted training, preventive maintenance, contingency planning, and well-directed training to systematic preventive maintenance and the careful establishment of contingency arrangements. Resistance, in turn, reflects the system's ability to maintain stability in the face of an initial shock, ensuring that performance remains above a critical threshold. When the disturbance exceeds the limits of that resistance, the absorption phase becomes critical. At this stage, the emphasis shifts to the system's ability to curb the fall in performance, contain the damage, and withstand the inevitable impacts of the disruption—thereby avoiding a complete operational collapse. Its speed and effectiveness depend on both internal (resources, redundancies, technical capabilities) and external (support, logistics, operating environment) factors. Adaptation reflects the system's capacity to learn, improve, and potentially exceed prior performance, confronting future challenges with greater mettle.

© Editorial Académica Dragón Azteca S. de R.L. de C.V. (EDITADA.ORG), All rights reserved.

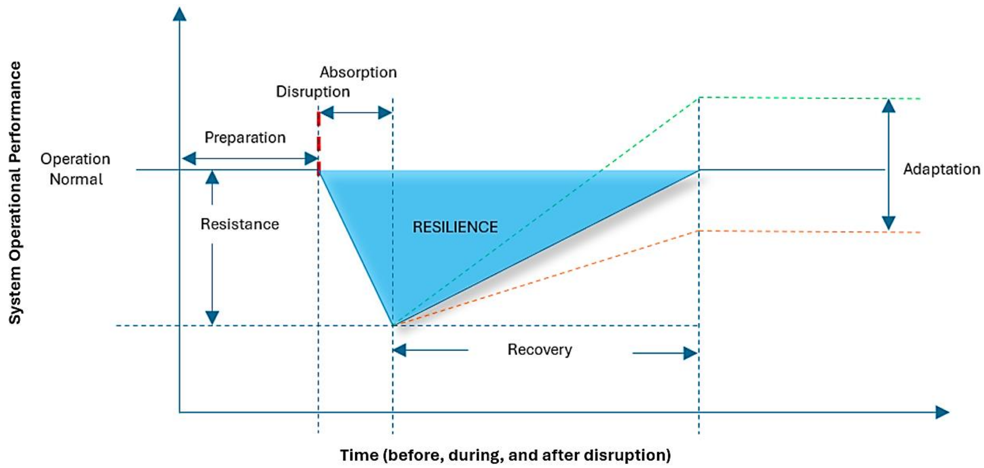

Fig. 1. Stages of Resilience. The horizontal axis represents time, and the vertical axis indicates the supply chain's operational efficiency. The arrows illustrate the magnitudes associated with the concepts used to model resilience. Adapted from Yang et al. (2022).

In addition, resilience provides a significant competitive advantage. Organizations that can identify vulnerabilities in their supply chains can implement proactive strategies, such as supplier diversification, strategic warehousing, or the creation of flexible logistics networks (Sheffi, 2015). This not only reduces the impact of adverse events but also improves overall system efficiency and adaptability, enabling it to meet customer expectations better and maintain the company's reputation (Christopher & Peck, 2004). Resilience analytics also contributes to cost optimization. By anticipating potential outages and preparing for them, businesses can avoid unforeseen expenses associated with material shortages, price spikes, or extended downtime. This enables more stable and predictable supply chain operations, facilitating more accurate financial planning and efficient allocation of resources (Waller & Fawcett, 2013). Finally, within the context of sustainability and corporate responsibility, resilience strengthens companies' ability to operate ethically and socially responsibly. Resilient supply chains not only protect the organization's financial interests but also promote practices that benefit communities and reduce environmental impact. Consequently, companies can ensure a balance between economic growth, social welfare, and sustainability, positioning themselves as leaders in their respective industries (Negri et al., 2021). Therefore, this study develops a dynamic methodology to uncover the multi-effect structure of resilience in the supply chain, that not only measures resilience but also provides evidence that interactions among the Synchronization, Spillover, Bullwhip, Ripple, and Economics effects effectively captures the behavior of effect Supply chain resilience, highlighting the complex interdependencies that shape its dynamics.

This research is structured as follows: Introduction (Section 1), Experimental procedures (Section 2), Results (Section 3), and Conclusion (Section 4).

1.1 Resilience structural behavior in supply chains

Based on a literature review structured using Web of Science data (Clarivate) for the period 2000 - 2024, and using keywords such as "Resilience", "supply chain", "disruption", 49 studies were identified: 9 studies were excluded due to limited accessibility, some of them do not address the structure dynamics of resilience: (Rajesh et al., 2015), (Mari et al., 2015); some of them approach structure of resilience indirectly, and only from the analysis of disruption occurrence and risk (Lorenc & Kuznar, 2021; Friday et al., 2021; Zheng et al., 2023). Based on this, we derive the following classification of ways to analyze structural resilience in a Supply Chain: qualitative and quantitative research. This approach ensures that the categorization is replicable and robust because qualitative and quantitative methods are established standards in scholarly studies (Silverman, 2016). This structured approach enhances resilience analysis across methodologies. Using these approaches, the classification results shown were obtained in Table 1.

Table 1. Comparatives resilience studies, showing their opportunities.

Study	Opportunity Area
Browning et al. (2022)	Needs further exploration of the resistance and absorption stages, especially in the face of unforeseen disruptions.
Olivares et al. (2021)	Opportunity to explore absorption and recovery stages more deeply.
Ivanov (2021)	Limited focus on recovery and adaptation, areas that could benefit from more forecasting.
Bathke et al. (2021)	Underexplored preparation and adaptation forecasting.
Wide (2020)	Could expand to preparation and adaptation, especially for long-term resilience.
Ivanov et al. (2020)	Needs more research on the recovery and adaptation stages to enhance understanding of resilience.
Rajagopal (2016)	Needs further exploration of preparation and adaptation stages to improve early and long-term resilience.
Zeng & Yen (2016)	Opportunity to expand resilience forecasting to recovery and adaptation stages.
Rajesh et al. (2015)	It could be expanded to include the preparation, recovery, and adaptation stages.
Gupta et al. (2022)	Underexplored recovery and adaptation, which could further improve supply chain resilience.
Nagy & Foltin (2022)	It could benefit from analysis in preparation, recovery, and adaptation stages.
Wang et al. (2017)	Focused on recovery and adaptation could be further developed with more advanced forecasting techniques.
Wang et al. (2020)	Needs more exploration of preparation and recovery stages in forecasting resilience.
Ghafour & Aljanabi (2023)	Needs to explore preparation, recovery, and adaptation stages more deeply for resilience.
Chowdhury (2015)	It could expand to preparation, recovery, and adaptation stages for a more holistic approach.
Hsu et al. (2022)	Limited focus on preparation and adaptation, with more focus on operational resilience.
Cavalcante et al. (2019)	Could benefit from additional analysis on the preparation and adaptation stages.
Chukwuka et al. (2023)	Could include preparation and recovery stages to enhance understanding of resilience.
Behera & Ramanathan (2022)	Focused on recovery, could expand to preparation and adaptation stages for more comprehensive resilience.
Gružauskas & Burinskiene (2022)	Needs more exploration of preparation and adaptation stages to complete the resilience forecasting cycle.
Rajesh (2019)	It could benefit from more detailed analysis in the preparation and recovery stages.
Rajesh & Rajendran (2019)	Opportunity for further analysis in adaptation forecasting.
Gultekin et al. (2022)	Could benefit from further exploration of preparation and adaptation stages.
Lorenc et al. (2021)	Could expand to preparation and adaptation stages for a broader view of resilience.
Ramsey et al. (2020)	Opportunity for further exploration in the preparation and adaptation stages.

A closer examination of the studies listed in Table 1 allows for a more precise positioning of the present work within the existing literature. Browning et al. (2022) employ a qualitative, scenario-based framework to explore preparation and adaptation strategies in supply chains. While providing detailed contextual narratives, their approach lacks predictive mechanisms for resistance and absorption stages, thereby leaving a gap addressed by our methodology through integrated, data-driven dynamics across all stages. Olivares et al. (2021) similarly focus on preparation and adaptation through survey-based resilience assessments, but do not extend their analysis to recovery modelling; our framework explicitly links early-stage readiness with post-disruption recovery dynamics. Ivanov (2021) presents a simulation-based quantitative model incorporating Ripple and Bullwhip effects during resistance and absorption. However, it omits Synchronization and Spillover effects, and does not account for preparation or adaptation stages. In contrast, our approach captures the complete set of logistics resilient effects while modelling dynamic transitions between all resilience stages. Bathke et al. (2021) and Wide (2020) concentrate on absorption and recovery, mainly using post-event performance metrics. While valuable for benchmarking, these studies remain reactive; our work integrates a comprehensive resilience framework across different disruptions, thereby supporting both preventive and corrective resilience strategies.
Several studies—such as Rajagopal (2016), Zeng & Yen (2016), and Rajesh et al. (2015)—apply qualitative or mixed-method risk assessment frameworks to assess resistance and absorption. These provide important descriptive insights but lack the predictive depth required for early warning or cross-stage transition modelling. Our methodology advances these approaches by quantifying resilience and enabling structural analysis using heterogeneous data.

Gupta et al. (2022) represent one of the few works integrating economic factors into resilience modelling, but their scope remains sector-specific and partial in its inclusion of logistics effects. Our work generalizes across sectors and combines economic variables with Synchronization, Spillover, Bullwhip, and Ripple effects. Similarly, Nagy & Foltin (2022), Wang et al. (2017, 2020), Ghafour & Aljanabi (2023), and Chowdhury (2015) examine resistance and absorption using sector-focused empirical datasets, yet omit preparation, recovery, or adaptation modelling—gaps that our cross-stage approach directly addresses.
Studies like Hsu et al. (2022), Cavalcante et al. (2019), Chukwuka et al. (2023), Behera & Ramanathan (2022), and Gružauskas & Burinskiene (2022) provide valuable case-study-driven analyses of disruptions. However, their emphasis on individual phases—often recovery or absorption—precludes an understanding of the resilience cycle as a whole. By contrast, this study integrates the full dynamics of resilience in a unified structural model, enabling decision-makers to anticipate and manage resilience transitions holistically.

Rajesh (2019) and Rajesh & Rajendran (2019) expand coverage to include preparation and recovery, using structured frameworks that improve breadth but still lack complete adaptation modelling and integration of multiple disruption effects. Gultekin et al. (2022), Lorenc et al. (2021), and Ramsey et al. (2020) similarly present partial stage coverage with limited methodological integration. Our approach overcomes these constraints by embedding non-linear modelling techniques to capture the complex interplay between effects and resilience.

This detailed comparison underscores two key differentiators of the present work: (1) comprehensive stage coverage of resilience versus the partial coverage of prior studies, and (2) integration of five significant logistics effects within a unified, non-linear analysis and structural behavior framework, enabling both proactive and reactive resilience management.

As shown in Table 1, most studies address only a subset of effects on resilience. Quantitative approaches are more common in later stages, whereas early phases often rely on qualitative methods. Across the literature, there is no single framework that integrates resilience with multiple logistics effects, leaving significant gaps in structural capabilities for long-term and unforeseen disruptions.

While Table 1 provides a mapping of methods across resilience stages, the distribution of studies also reveals structural and systemic reasons behind these gaps. One major cause is the uneven availability of data across resilience effects. This asymmetry naturally drives researchers toward certain phases while leaving others underexplored.

A second factor is methodological path dependence. Many studies extend established models—often linear and phase-specific—because these approaches are well documented, less resource-intensive, and easier to validate. However, such incrementalism discourages the development of integrative frameworks capable of capturing transitions between effects. The persistence of linear modelling prior to the recent maturation of AI/ML (Artificial Intelligence/Machine Learning) also limited the ability to represent the non-linear interplay between disruption effects and resilience responses.

Third, research funding and policy priorities have historically favored immediate post-event recovery over long-term resilience planning. Projects with visible short-term impact, such as restoring operations after a disruption, are more likely to receive institutional support than studies that focus on less tangible pre-event capacities. This incentive structure reinforces the bias toward later stages of the resilience cycle. Furthermore, sector-specific constraints—such as confidentiality in defense supply chains or proprietary data in pharmaceuticals—can make it challenging to build multi-stage, cross-sector datasets, further entrenching fragmented research patterns.

These structural conditions have important consequences. If key logistics effects are overlooked, resilience models may produce incomplete or even counterproductive recommendations. For example, overemphasizing recovery without sufficient Synchronization modelling may lead to reactive rather than proactive strategies, increasing vulnerability to future disruptions. Similarly, neglecting the simultaneous impact of multiple logistics effects—such as Spillover disruptions, or the Bullwhip and Ripple effects—can underestimate systemic risks and overstate a supply chain's true resilience.

The present work directly addresses these dynamical relationships and consequences by introducing the resilience velocity construct, which enables time-sensitive measurement of resilience transitions across all stages. It also integrates five key logistics effects (Synchronization, Spillover, Bullwhip, Ripple, and economic effects) into a unified, non-linear structural framework. Leveraging machine learning capable of handling heterogeneous data, this approach transcends the historical constraints on cross-stage analysis. In doing so, it closes the descriptive–predictive gap identified in Table 2 and provides a decision-support tool that can inform both immediate response and long-term resilience planning.

Although several prior works have attempted to include multiple disruption effects in resilience analysis, none have achieved the level of integration and scope proposed here. For example, Ivanov (2021) incorporates Ripple and Bullwhip effects into a disruption propagation model but focuses mainly on mid-cycle stages (resistance, absorption) and does not address Synchronization, Spillover, or the complete transition across all resilience stages. Gružauskas and Burinskiene (2022) combine Ripple effects with recovery dynamics. However, their scope is restricted to post-disruption phases, omitting preparation and adaptation, and excluding key effects such as Synchronization and economic behavior. Gupta et al. (2022) integrate some interdependencies between disruption effects and economic factors, but the approach is sector-specific and does not generalize across industries or model the complete resilience cycle.

Although the primary objective of this study is to understand supply chain resilience as a multi-effect dynamic phenomenon rather than to develop a methodology per se, it is important to position the analytical approach used in relation to existing literature. While no prior study provides an integrated framework that simultaneously captures multiple logistics effects across all resilience stages, the literature does employ distinct methodological approaches to analyze partial aspects of the phenomenon. These include simulation-based models that explore disruption propagation dynamics, econometric and spatial models that capture spillover and structural relationships, machine learning approaches focused on prediction and pattern recognition, and qualitative or survey-based frameworks that provide contextual and strategic insights. However, these approaches remain fragmented, typically addressing isolated effects or specific stages of resilience. This fragmentation highlights a methodological gap that justifies the integrated, nonlinear, and multi-effect framework proposed in this study, which is designed to capture the dynamic interactions underlying resilience as a unified process.

The primary contribution of this framework is that it brings together five significant logistics effects—Synchronization, Spillover, Bullwhip, Ripple, and economic—into a unified, non-linear structural behavior that explicitly models the dynamic transitions across resilience. Machine learning techniques are not the primary contribution but serve as an enabling mechanism but as an enabling mechanism that allows this unprecedented integration to operate on heterogeneous data streams. This design closes both the methodological gap in multi-effects modelling and the stage coverage gap identified in prior literature, delivering a framework that is both broader in scope and deeper in its capacity to capture the complexity of global supply chain resilience.

Table 2. Comparative summary of prior multi-effects resilience models versus the proposed framework, highlighting differences in the scope of logistics effects, coverage of Resilience, and remaining limitations.

Study	Logistics effects included	Main limitations
Ivanov (2021)	Ripple, Bullwhip	No Synchronization or Spillover effects; omits preparation and adaptation; limited cross-stage dynamics.
Gružauskas & Burinskiene (2022)	Ripple	Post-disruption focus only; omits preparation, resistance, and adaptation; excludes Synchronization, Spillover, Bullwhip, and economic effects.
Gupta et al. (2022)	Economic (partial), Bullwhip (implicit)	Sector-specific; incomplete effect integration; does not cover the complete resilience cycle.
Proposed framework	*Synchronization, Spillover, Bullwhip, Ripple, Economics*	—

Analysis of the studies summarized in Tables 1 and 2 reveals three recurrent methodological limitations in resilience literature. First, most prior work relies on linear modeling approaches that cannot fully capture the complex, non-linear interdependencies among resilience drivers. Second, existing metrics tend to assess static end-state outcomes rather than time-sensitive trajectories. The present study addresses these gaps by introducing the resilience velocity construct, which explicitly measures the rate of change in resilience over time; by integrating multiple effects within a non-linear framework based on Transfer Entropy to capture dynamic interdependencies; and by analyzing the complete resilience cycle across different disruption regimes. This integrated approach overcomes prior methodological constraints, yielding a broader understanding of resilience dynamics and advancing resilience scholarship by linking identified gaps to this study's innovations.

It is worth noting that several of the most recent studies on AI/ML and resilience forecasting, while not meeting the specific inclusion criteria for Table 2, provide valuable methodological and contextual insights. Despite being outside the scope of the table's classification framework, these studies illustrate how recent advances still leave unaddressed gaps that our multi-effect, multi-stage methodology aims to fill. Recent post-2020 studies have markedly advanced AI/ML-based resilience forecasting, particularly in the context of pandemic-scale disruptions. Salehi, Babaei, and Hamidi (2025) suggested combining AI, IoT, and digital twins to handle pandemics. In 2024, PandemicLLM, a real-time forecasting model merging diverse data sources, was launched. Consequently, Zogaan, Ajabnoor, and Salamai (2025) improved demand prediction and inventory management in sectors such as pharmaceuticals, automotive, and agriculture using deep learning (RNNs, LSTMs, GRUs, CNNs, and ANNs). Al-Hourani and Weraikat (2025) reviewed AI/ML in pharmaceutical supply chains, mapping resilience dimensions and identifying gaps in regulation and deployment.

These advances underscore the growing role of AI/ML in resilience analysis. However, they share common limitations: most focus on specific sectors, often model only part of the resilience process, and seldom account for the simultaneous impact of multiple logistics effects. In contrast, the present study—while leveraging ML techniques for structural analysis—pursues a broader objective: it integrates five distinct logistics effects (Synchronization, Spillover, Bullwhip, Ripple, and economic effects) into a unified, non-linear resilience structural framework, contributing by integrating these mechanisms within a unified hierarchical framework. This integrated approach addresses the identified methodological gaps. It also enables the model to capture the complex, multi-effect and multi-stage nature of resilience in global supply chains—using the maritime port system as a high-impact, data-rich case study to validate the model.

Based on the evidence presented in Table 2, a holistic and multidisciplinary methodology is appropriate, well justified, and aligned with current scientific practices in supply chain research. Several foundational studies demonstrate that the complexity of modern supply chains requires integrating multiple decision layers (strategic, tactical, and operational) and combining methods from disciplines such as economics, engineering, finance, sustainability, and mathematical optimization. For instance, Erlebacher and Meller (2000) and Elhedhli and Gzara (2008) adopt integrated approaches to jointly address facility location, inventory management, and technology selection, underscoring the need for models that cross traditional disciplinary boundaries. Similarly, Farjana Nur et al. (2021) illustrate how incorporating agronomic, logistics, and sustainability dimensions into a stochastic framework significantly enhances decision robustness.

Several studies have demonstrated the value of integrated and quantitative approaches to address complex coordination and design challenges in supply chains. Moses and Seshadri (2000) use game theory and deferred payment contracts to model inventory coordination between manufacturers and retailers, showing how financial incentives can align decentralized decisions with system-wide optima. Zhao and Wang (2002) address double marginalization in decentralized channels by modeling joint pricing and production decisions as a dynamic bilevel game and show that a time-based wholesale pricing scheme can achieve perfect coordination. Meanwhile, Zhang and Zhang (2019) integrate location, pricing, and inventory decisions in a supply chain handling both new and remanufactured products, accounting for demand cannibalization. Their nonlinear model is reformulated as a second-order cone program and solved via outer approximation, revealing that ignoring cannibalization results in suboptimal network designs. Collectively, these studies validate hybrid methodologies that combine economic theory, operations Engineering, and advanced optimization to solve real-world coordination and efficiency problems in complex logistics systems.

Moreover, the phenomena studied in these works—strategic channel coordination, cannibalization effects, decision-making under uncertainty, and incentive alignment—cannot be effectively addressed through single-discipline approaches. Authors such as Nembhard et al. (2005) and Gang Li and Yu (Amy) Xia (2023) explicitly develop hybrid frameworks that combine financial theory, operations management, and sustainability goals, using tools such as real options analysis and multi-objective models incorporating ESG indicators. This empirical and methodological support confirms that adopting a holistic approach in our research is neither incorrect nor arbitrary—it reflects a scientific shift toward integrative and cross-disciplinary models capable of capturing the multifaceted nature of supply chain systems.

Additionally, the model developed in this research is grounded in the identified opportunity areas. Accordingly, the proposed algorithm is designed to integrate resilience, together with the Synchronization effect. It also incorporates a nonlinear representation of the Spillover effect to better capture its complexity and impact. Furthermore, the algorithm includes the Bullwhip and Ripple effects, while embedding social, decisional, and economic variables within the SCR framework. Finally, the methodology accounts for the economic behavior associated with each type of disruption during the resilience process by incorporating the corresponding constraints.

International Journal of Combinatorial Optimization Problems and Informatics, 17(4), 2026, 180-204. ISSN: 2007-1558.
https://doi.org/10.61467/2007.1558.2026.v17i4.1317
www.editada.org

2 Experimental procedures

2.1 The concept

The strategy implemented to represent resilience, together with the aforementioned effects such as Synchronization, Spillover, Bullwhip, Ripple, and economic effects, is that resilience is a velocity-driven outcome resulting from the interaction of these effects over time. These interconnected dynamics are visually represented in Figure 2, which presents the conceptual interaction map underlying our model of resilience velocity. This diagram synthesizes the five effects—Synchronization, Spillover, Bullwhip, Ripple, and Economic Effects—and their hypothesized bidirectional contribution on each other and on the resilience velocity construct. Each effect may have either a positive or negative impact depending on the stage of Resilience (preparation, absorption, recovery, adaptation) and the context. This framework positions resilience velocity not as a static, additive outcome but as an emergent property of a dynamic, stage-dependent network of interactions.

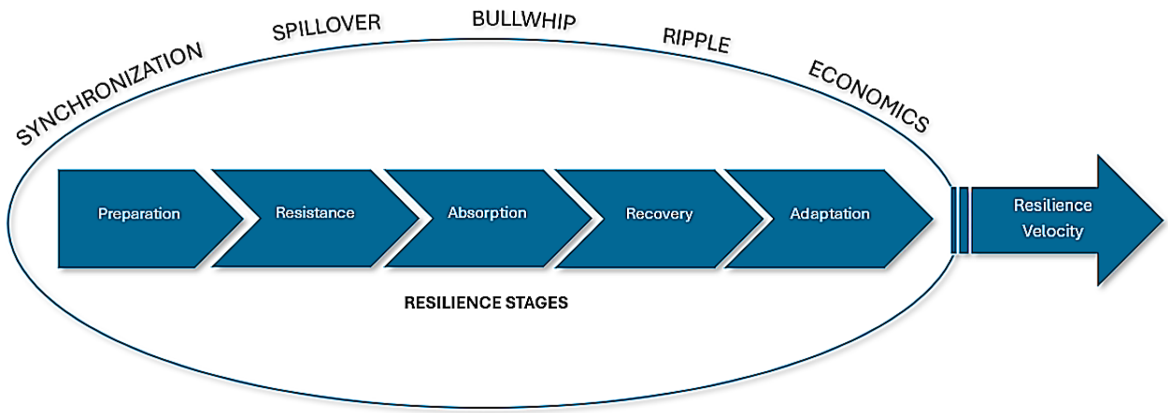

Fig. 2. Conceptual interaction map of five resilience effects—Synchronization, Spillover, Bullwhip, Ripple, and Economic—and their bidirectional, context-dependent contribution on resilience velocity, underscoring the model's dynamic, non-additive nature.

In this study, we define "resilience velocity" as the relative rate of time change in a supply chain's operational performance during the recovery trajectory following a disruption, regarding the mutieffect scope (Synchronization, Spillover, Bullwhip, Ripple, and economics). Although a more descriptive term could be used, "resilience velocity" is adopted for brevity". By modelling this derivative, we capture the phenomenon's dynamic nature from a practical standpoint, as with any other process. This construct is conceptually aligned with the resilience literature that distinguishes between the magnitude of resilience and its temporal dimension (Hosseini et al., 2019; Sheffi, 2015). While traditional metrics focus on end-state recovery levels, resilience velocity captures how quickly the system progresses through the resilience stages (preparation, absorption, recovery, adaptation) after a disturbance. This temporal emphasis responds to calls in resilience theory for dynamic indicators that reflect system responsiveness and adaptability over time (Ponomarov & Holcomb, 2009; Chowdhury et al., 2021). By situating velocity within established resilience theory, our approach extends existing models from static, event-focused assessments to a continuous, time-sensitive framework. In light of the above, we propose the next reduced-form state equation model [1], which expresses the resilience velocity $C_{i,t}$ as the sum of three components: a nonlinear structural term $S(X_{i,t}, \gamma)$, representing supply rhain resilience, driven by relative changes in system variables, a memory term $\alpha[C_{i,t-1} - S(X_{i,t-1}, \gamma)]$ capturing temporal persistence and adjustment dynamics, and a latent exogenous shock $\beta_i Z_{i,t}$ representing unobserved systemic perturbations. The structural component encodes nonlinear interactions among drivers and the memory parameter. α governs the contribution of past deviations from structural equilibrium, and the idiosyncratic loading β_i allows heterogeneous responses to standard exogenous shocks across units, while the residual term accounts for unexplained variability.

$$C_{i,t} = S(X_{i,t}, \gamma) + \alpha[C_{i,t-1} - S(X_{i,t-1}, \gamma)] + \beta_i Z_{i,t} + \varepsilon_{i,t} \quad [1]$$

© Editorial Académica Dragón Azteca S. de R.L. de C.V. (EDITADA.ORG), All rights reserved.

The present study is framed within a resilience-disruption analysis, aimed at characterizing the port system during disruptive events—the 2008–2010 & 2020-2023 crisis periods. With this framework, model-derived projections support port planning and management, as they provide approximate estimates of the potential impacts of future external shocks and help prepare mitigation and response strategies.

2.2. The model

2.2.1. For the representation of the multi-effects behavior of resilience Velocity

For three reasons, we use resilience velocity as our primary performance measure. First, it measures how well the system adapts in a consistent, comparable way across disruptions of different sizes. Second, it accounts for both the size and the duration of resilience phases, a problem with metrics that do not factor in time. Third, it provides us with one way to see how different systemic effects, such as synchronization, spillover, bullwhip, ripple, and economic factors, interact over time. This method is more than just a simple scoring system; it shows you how effects interact in ways that are not always straight lines and depend on the stage.

The model must simultaneously represent the five effects indicated above (Synchronization, Spillover, Bullwhip, Ripple, and economic effects), as described in the following development: The concept of risk prevention in a supply chain is derived from the field of Risk Management (Aven, 2015). This preventive work (*lp*) for each link in the supply chain can be represented as the rate of preventive work (φ) that anticipates risk, which must vary over time (*t*). Moreover, it should be proportional to production flow Γt (the tonnage shifted in maritime port) as given by [2]:

$$lp_t = \frac{\frac{d\Gamma}{d_t}}{\Gamma_t}\left(1 + \frac{\frac{d\varphi}{d_t}}{\varphi_t}\right) \qquad [2]$$

This rate is, in turn, contributed by the level of advantages gained in the supply chain due to the generated Synchronization (Λ), as well as by the level of Spillover (Φ) at their respective rates, represented as [3]:

$$lp_t = \frac{\frac{d\Gamma}{d_t}}{\Gamma_t}\left(1 + \frac{\frac{d\varphi}{d_t}}{\varphi_t}\right)\left(1 + \frac{\left(\frac{d\Lambda}{dt}\right)}{\Lambda_t} - \frac{\left(\frac{d\Phi}{dt}\right)}{\Phi_t}\right) \qquad [3]$$

Note that in [3], when the level of Synchronization and positive spillover equals the observed level of risk, the links in the supply chain will reduce their risk requirements. Additionally, Synchronization is assigned a positive sign, indicating that the closer it is to zero, the more favorable it is for the preventive labor rate, as Synchronization reduces differences between systems. Regarding the Spillover effect, it is applied with a negative sign to indicate that the more positive the effect, the better it is for the subscript base, *lp*, as the Spillover effect can be either beneficial or adverse. Furthermore, SCR extends beyond the disruption period, with its rate of reduction or depreciation composed of the variation rates of two adverse effects on performance of resilience (*R*) and the transmission of information between links in the supply chain, namely the Bullwhip effect (*W*) and the Ripple effect (*D*) [4]. This is part of the growth in investment in maritime port assets (Ω), which are used by system actors to mitigate risk from disruptive risks:

$$\Omega_t = \frac{\frac{dR}{dt}}{R_t}\left(1 - \frac{\left(\frac{dW}{dt}\right)}{W_t}\frac{\left(\frac{dD}{dt}\right)}{D_t}\right) \qquad [4]$$

In [4], it should be noted that the relative growth of the Bullwhip effect (*W*) is negative, as it reflects a market fracture in its information transmission mechanisms. Additionally, it is important to highlight that the relative growth of this Bullwhip effect is a function of the Ripple effect (*D*) acting as a multiplier, since the Ripple effect can accelerate the Bullwhip effect. Now, with the same resources, and based on the fact that a company can implement its resilience strategies proactively (such as preventing inventory shortages, establishing agreements with suppliers in the event of disruptions, etc.), these actions are represented by *lp*. Similarly, a company can also adopt reactive resilience strategies (such as investing in specialized machinery once a disruptive event is identified), represented by Ω. Therefore, the following equality is proposed in [5]:

$$lp = \Omega \qquad [5]$$

Applying [5], in [3] and in [4] an equality is obtained, to give rise to [6]:

$$S = \frac{\dot{R}}{R_t} = \frac{\gamma_\Gamma \frac{\dot{\Gamma}_t}{\Gamma_t}\left(1 + \gamma_\varphi \frac{\dot{\varphi}_t}{\varphi_t}\right)\left(1 + \gamma_\Lambda \frac{\dot{\Lambda}_t}{\Lambda_t} - \gamma_\Phi \frac{\dot{\Phi}_t}{\Phi_t}\right)}{\left(1 - \gamma_W \frac{\dot{W}_t}{W_t} \gamma_D \frac{\dot{D}_t}{D_t}\right)} \qquad [6]$$

Where Bullwhip effect (*W*) and Ripple effect (*D*) is shown, the rate of preventive work (φ) that anticipates risk which must vary over time (*t*), the generated Synchronization (Λ) which is obtained by [10], the level of Spillover (Φ), all variables are dynamically proportional to time. With Equation [6], we deliberately inserted behavioral parameters into each variable and successfully captured the behavior of rupply chain resilience (*S*) as a result of synchronization, Spillover, Bullwhip, Ripple, and economic effects. Additionally, this result provides a useful tool for analyzing the behavioral nature of supply chain resilience over a given period. Although Equations [1] – [6] set out the formal mathematics of the model, the underlying concepts can be explained more intuitively: Equation [1] captures the resilience of a system's usual activity—such as cargo throughput—that is lost during a disruption, along with the pace of recovery, while factoring in the impact of earlier disruptions. Equations [2] and [3] illustrate how preventive strategies and collaborative efforts among system actors—via Synchronization and Spillover—enhance the capacity to anticipate and mitigate risks. Equation [4] explores how market distortions—known as the Bullwhip effect—can destabilize the system, and how these disturbances intensify as they spread through network connections, a phenomenon referred to as the Ripple effect, ultimately impacting investment forces. Equation [5] distinguishes between proactive and reactive resilience strategies, fighting at the same level. At the same time, Equation [6] integrates all these effects into a single dynamic measure—resilience velocity—that captures how quickly the system is moving back toward resilient stability. In simple terms, the model conceptualizes resilience as a dynamic recovery process: some factors act like tailwinds (positive Spillover, good Synchronization), while others act like headwinds (Bullwhip, Ripple), and the resulting instantaneous rate of change is what we call resilience velocity.

Although Equation [6] summarizes the model in a compact form, the estimation process does not treat the five effects as static, independent add-ons. Each effect's contribution is estimated dynamically over time through the particle filtering framework, which adapts coefficients in response to stage-specific conditions (Absorption, Recovery, Adaptation). Moreover, some effects inherently interact—for instance, the Bullwhip effect modulates and is modulated by the Ripple effect, while Synchronization can amplify positive Spillover gains. These interdependencies mean that resilience velocity emerges from evolving relationships among the effects, rather than from a fixed additive structure. The term "resilience velocity" is used here in a strict analytical sense, referring to the time derivative of Resilience with respect to the multieffect interactions; in other words, it captures the rate of change of the system's resilience over time. Figure 2b illustrates these dynamic, stage-dependent interactions, making explicit the cross-effect contributions already embedded in the model's structure.

A computational framework is developed that integrates Bayesian optimization, dimensionality reduction, machine learning, and particle filtering to enhance the estimation of resilience velocity. Bayesian optimization is employed instead of traditional methods such as gradient descent or random search, as it efficiently explores high-dimensional spaces while requiring fewer costly objective function evaluations. Additionally, a regularization term is incorporated to mitigate overfitting and stabilize parameter optimization. Furthermore, Principal Component Analysis (PCA) is used for dimensionality reduction, avoiding arbitrary variable elimination or manual feature selection, thereby preserving the most relevant data structure while avoiding loss of critical information. To determine each type of effect, we used the next models:

www.editada.org

International Journal of Combinatorial Optimization Problems and Informatics, 17(4), 2026, 180-204. ISSN: 2007-1558.
https://doi.org/10.61467/2007.1558.2026.v17i4.1317

2.2.2. Inter-relationship analysis

a) For the representation of resilience

To accurately capture resilience behavior at each stage, it is essential to first establish a general representation of the gross resilience. This representation is mathematically expressed through our proposal steps, starting with the given normal reference-level for resilience in the *t*=0 for disruption [7.1]:

$$B = \ median\{\Gamma_{-k}\}_{k=1}^{N} \quad [7.1]$$

Where Γ denotes the tonnage shifted before the disruption (effect with a N =11-month period, applied in this study for practical purposes). This B helps to detect when the resilience is reaching out to the normal level in whatever time in Γ, measuring the tonnage productivity compared to the base level. We applied the median statistic to smooth the outliers, which a simple average cannot handle well. Once we got B, we need to know how much deviation there is over time in the productivity of the tonnage to reach the level of B, by means of [7.2]:

$$\omega_t = \Gamma_t - B \quad [7.2]$$

where if $\omega_t < 0$ means that the system is in the stage of resistance and/or absorption of the given disruption (tonnage deficit), and if $\omega_t \approx 0$ means that the system is already very close to the B level, implying that it has already predominantly passed through the recovery and/or adaptation stage. With ω_t, we can insert the "point to be reached during all disruption time", of the exact nature as the resilience itself. Now, we define the net cumulative impact [7.3] (because reality allows high peaks that can compensate for losses, over time):

$$R_t = \frac{\omega_t - \omega_{t-1}}{\omega_{t-1}} \quad [7.3]$$

where we observe that if $R_t < 0$ means that up to the given time t, the system is in tonnage loss; if $R_t = 0$ the system is close to or in equilibrium to full resilience; and if $R_t > 0$ means that the system is already in an accumulation gain adaptation. It should be noted that this is a relative growth, and it is necessary to apply it because in this way we are respecting the speed with which the resilience of each seaport moves, regardless of its tonnage. After all, this way its intrinsic port capacity for each one is respected. Finally, we obtain a time series that is representative in terms of structure and form of resilience.

To better understand equations 7.1, 7.2, and 7.3, the following analogy focused on cooking temperature can be used: "B" represents the ideal temperature required to prepare a specific dish, while "ω" works like a thermometer, indicating how hot or cold the current temperature is relative to that ideal level. However, a thermometer only provides a snapshot at a given moment. That is why we need a "pressure cooker", R, which helps determine when the ideal temperature is actually achieved over time, taking into account both previous variables. This dynamic, intertemporal temperature is ultimately what ensures the perfect consistency of the dish (Figure 3).

It is necessary to highlight that although this study offers its own novel proposal for the measurement of resilience, this measurement is not the main objective of the study, but, as described above, it is about how the effect of resilience is represented by the multi-interaction of logistic effects such as Synchronization, Spillover, Bullwhip, Ripple, and Economic effects.

© Editorial Académica Dragón Azteca S. de R.L. de C.V. (EDITADA.ORG), All rights reserved.

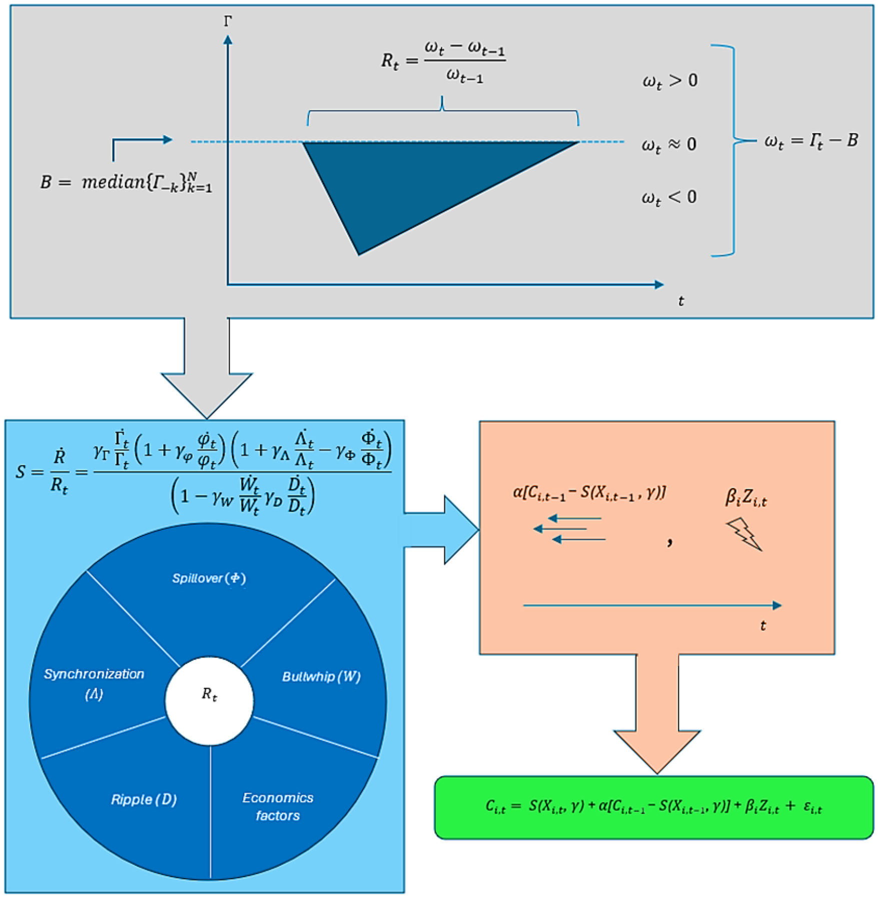

Fig. 3. Intuition Behind the Model: A Visual Approach.

b) Synchronization

Based on the model presented by Göksu et al. (2014), to represent Synchronization in a supply chain, we express it using the following system of equations [8.1, 8.2, 8.3]:

$$\frac{dx_1}{dt} = (m + \delta m)y - (n + 1 + \delta n)x + d_1 \qquad [8.1]$$

$$\frac{dy_2}{dt} = (r + \delta r)x - y - xz + d_2 \qquad [8.2]$$

$$\frac{dz_3}{dt} = xy + (k - 1 - \delta k)z + d_3 \qquad [8.3]$$

where *x, y, z* represents demand, inventory, and production, respectively; *m, n, r, k* represents constant parameters of delivery efficiency, demand/customer ratio, inventory distortion, and inventory safekeeping, respectively; δ represents a linear perturbation parameter, and d_n represents a nonlinear perturbation for each state variable. Now, the proposal for the present Synchronization model research is described below, inserting in x as Γ (tonnage handled by seaport, see [2]); inserting in *y* as *Q* (level of intensity in overuse of seaports), and *z*, such as the ratio of the tonnage handled by seaport, with respect to the level of intensity in overuse of seaports, obtaining the efficiency of those inputs. Now, for our research, we selected the ports of the Pacific-Central Zone as an element of control of the port network, since the most important port in Mexico (Port of Manzanillo) is located in that area. This control system represents a system composed of x_2, y_2, z_2, and the rest of the port areas to be controlled are represented x_1, y_1, z_1. By subtracting these systems, a resulting difference is obtained, which tends to zero when the Synchronization phenomenon is achieved, thus obtaining [9.1,9.2,9.3] and [10.1,10.2,10.3]:

$$\dot{e}_1 = (m + \delta m)e_2 - (n + 1 + \delta n)e_1 \quad [9.1]$$
$$\dot{e}_2 = (r + \delta r)e_1 - e_2 - x_2\Gamma_2 + x_1\Gamma_1 \quad [9.2]$$
$$\dot{e}_3 = x_2y_2 - x_1y_1 + (k - 1 - \delta k)e_3 \quad [9.3]$$

where:

$$e_2 = x_2 - x_1 \quad [10.1]$$
$$e_2 = y_2 - y_1 \quad [10.2]$$
$$e_3 = z_2 - z_1 \quad [10.3]$$

Note that by subtracting both systems, the random perturbation d_n is eliminated. In this research, the parameters *m, n, r, k* were obtained using of generalized least squares panel data (with statistically significant results evaluated in multicollinearity, autocorrelation, and heteroscedasticity) for each port zone (North Pacific Zone & Gulf of California, Central-South Pacific Zone, Gulf of Mexico Zone & Caribbean Sea).

c) Spillover

To obtain the Spillover effect, it is first necessary to define a model that represents the logistics-economic interaction in the port phenomenon. To this end, a production movement model is proposed and formulated using the following Cobb-Douglas model [11]:

$$\Gamma = K^{\alpha_1}L^{\alpha_2}Q^{\alpha_3}F^{\alpha_4}Z^{\alpha_5}e^{\lambda} \quad [11]$$

where Γ is port production (tonnage handled per seaport); K is the maritime port capital stock; L is the maritime port labor personnel; Q is the level of intensity in overuse of seaports (measured in empty containers); for this research, it applies the fact that the empty containers represent a real intensity over usage in supply chains, based on the next research: Dessouky (2020), Islam et al. (2019), Sáinz et al. (2016), Zhao et al. (2018); F is the average inflation level of the regions where the seaports are located; Z represent global exogenous phenomena of a disruptive nature affecting the maritime port sector (dichotomous variable); and e^{λ} is the exponential of the technological factor. For the case of the variable K, the following equation was applied to obtain it in order to represent the capital that is generated over time in each port in relation to its assets and infrastructure [12]:

$$K_t = \sum_{t=1}^{t} \frac{\zeta\eta}{\varsigma\phi}(1 - \Upsilon) \quad [12]$$

where ς is the "extension dock" port (kms), ϕ is the maritime investment made in the port (obtained by the Gross Domestic Product of the State where the maritime port is located , ζ is the Gross Domestic Product of the total regions where the seaport is located, η is the gross fixed investment generated at the national level, Υ is the depreciation rate of the said asset (for the present study, a depreciation rate of 15% per annum was applied to these port assets, based on port records (National Institute of Statistics and Geography [INEGI], 2024). Subsequently, spatial techniques, including the Spatially Lagged X's Model, the General nesting spatial model, and the Spatial error Durbin model, were applied, as they proved to be the most statistically significant spatial models for detecting spillover in the study time series across the different study panels.

d) Bullwhip effect

To measure the Bullwhip effect, the model described by Thomas and Mahanty (2019) was applied, based on the ratio between the variance of demand (DE) and the variance of consumption (CP). For our research and due to the lack of data in this regard, going back to Thomas & Mahanty and applying modifications for the present research, it is chosen to apply the ratio of expected demand over forecasted purchases according to the results of the surveys applied to the business sector of Mexico in the study period (INEGI, 2024), as well as its subtraction ratio against unity in its absolute value, which is presented as [13]:

$$BE = \left|1 - \frac{DE}{CP}\right| \quad [13]$$

e) Ripple effect

To measure the Ripple Effect, the "Beta" of the CAMP (capital asset pricing model) was used (Barberis et al., 2015), which captures financial systemic risk. However, for the present research, this logic was used to capture the supply chain's systemic risk, as shown in one of the first applications of this model in the logistics study. This Beta is represented as the relationship between the covariance of the Δ´s between two elements (study item & comparative item) with respect to the variance of the study item [14]:

$$\beta = \frac{covariance\ (\Theta, \mathrm{H})}{variance(\Theta)} \qquad [14]$$

where Θ represent the variation in production during port production (Γ), and H represents the variation in cabotage tonnage in the United States (comparator), since the United States is the market with the greatest impact on Mexico. For the economic impact analysis conducted in this research, an index was developed based on the logarithm of the directly proportional multiplication of the normalized GDP index and the normalized labor force index, while being inversely proportional to the Consumer Price Index (CPI), along with GDP and labor force, serves as key factors in the impact index, aligning with resilience and macroeconomic principles. GDP reflects economic health and capacity; higher levels indicate better resource mobilization for adaptation and recovery (Rose, 2004; Briguglio et al., 2009). The labor force signifies the pool of human capital that supports and sustains the absorption and adaptive capacities of supply chains (Hallegatte & Dumas, 2009). CPI captures inflationary pressures that can erode purchasing power, disrupt resource allocation, and increase operational costs, thereby slowing the recovery (Cavallo et al., 2016). In this study, GDP and the labor force are assumed to have positive effects on resilience, while CPI is assumed to have a negative effect, which aligns with findings in disaster economics and supply chain recovery research (Rose & Liao, 2005; Martin & Sunley, 2015). By incorporating these indicators in a normalized and combined form, the index captures the macroeconomic environment's net capacity to support or hinder resilience velocity. The values for each observation during the study period were obtained from the following data sources (see Table 3), and the summarization of all variables for the present study is on Table 4.

Table 3 Applied databases for study. Some variables used in the analysis—particularly macroeconomic indicators such as GDP and investment—are originally available at annual frequency. To ensure consistency with the monthly structure of the model, these variables were temporally disaggregated by assigning their annual values uniformly across the corresponding months (step-function approach). This approach is commonly used when higher-frequency data are unavailable and allows the variables to capture slow-moving structural effects without introducing artificial short-term volatility. Therefore, while the model operates at a monthly level, variables with annual frequency are interpreted as low-frequency drivers embedded within the dynamic system. For the estimation of variable ς, values were obtained from a technical source within the logistics sector (MexicoM Logistics, 2023), which provides specific operational information on container drayage in Mexican ports. This source was used due to the lack of systematized data in academic publications.

Variable	Data source used
Γ_t (tonnage shifted during the disruption)	Tons., (excluding oil and its derivatives) (Coordinación General de Puertos y Marina Mercante, 2007-2024)
φ (preventive work)	Manufacturing sector – Seasonally adjusted production expectations index (monthly, points), (INEGI, 2025a)
L (maritime port labor personnel)	Total employment by sector and domain – Index, deep-sea and cabotage traffic, (INEGI, 2025e)
F (average inflation level of the regions where the seaports are located)	National Consumer Price Index (INEGI, 2025f)
Z (global exogenous phenomena) (dichotomical variable)	0 = non-global exogenous phenomena) 1 = September, 2008 - December, 2009; January, 2020 – November, 2023)
ζ (Gross Domestic Product of the state where the seaport is located)	Gross Domestic Product by Federal Entity (GDP) (INEGI, 2024)
η (gross fixed investment)	Monthly Indicator of Gross Fixed Capital Formation (INEGI, 2025b)
ς (extension dock port , kms)	MexicoM Logistics (2023)
DE (variance of demand)	Expected order volume, Total manufacturing industries (INEGI, 2025c)
CP (variance of consumption)	Expected production volume, Total manufacturing industries (INEGI, 2025d)
(cabotage tonnage in the United States) to support for obtaining H	Tonnage for Internal U.S. Waterways, (U.S. Bureau of Transportation Statistics, 2025)

Table 4 Summarization of all variables and symbols used throughout the model. This unified notation ensures consistent interpretation across all equations and subsequent sections.

	Symbol	Definition
Indices and operators	i	Cross-sectional unit index
	t	Time index
	$\dot{x}$	Time derivative of variable x
	N	Number of observations (window size)
	k	Index for pre-disruption periods
Core model variables	$C_{i,t}$	Resilience velocity
	$S(X_{i,t}, \gamma)$	Structural resilience function
	$X_{i,t}$	Vector of explanatory variables
	γ	Structural parameter vector
	α	Memory parameter
	β_i	Unit-specific shock sensitivity
	$Z_{i,t}$	Latent exogenous factor
	$\varepsilon_{i,t}$	Error term
Resilience dynamics	R_t	Relative resilience change
	B	Baseline (median pre-disruption level)
	ω_t	Deviation from baseline
	ω_{t-1}	Lagged deviation
Logistics effects	Λ_t	Synchronization
	Φ_t	Spillover
	W_t	Bullwhip effect
	D_t	Ripple effect
Production and economic variables	Γ_t	Port production
	ϕ_t	maritime investment made in the port
	Ω_t	Reactive investment
	lp_t	Preventive labour
	K	Capital stock
	L	Labor
	Q	Utilization intensity
	F	Inflation
	Z	Exogenous dummy variable
	λ	Technology factor
	η	Gross fixed investment
	ζ	Regional GDP
	ς	Port infrastructure (dock length)
	Υ	Depreciation rate
Bullwhip and Ripple variables	DE	Expected demand
	CP	Expected consumption
	Θ	Variation in port production
	H	Variation in comparator system
Estimation framework	N_t	Number of particles
	ESS	Effective Sample Size
	w_t	Particle weight
	u_i	Unit-level random effect
	σ_γ^2	Variance of structural parameters
	σ_u^2	Variance of random effects
	$\mathcal{L}$	Loss function
	C^{sim}, C^{obs}	Simulated and observed resilience

The development of a hierarchical dynamic modeling system (Figure 3) amalgamates nonlinear structural dynamics, temporal memory, and external shocks to evaluate resilience velocity. It replicates this velocity through system variables, feedback mechanisms, and external shocks via a latent component. Parameter estimation uses hierarchical particle filtering, which takes into account both global and body-specific factors. Particle weights from a strong loss function with logarithmic squared residuals make the system more resilient. Stratified resampling with Effective Sample Size makes sure that stability and diversity are present. This approach elucidates common resilience mechanisms, local dynamics, and shocks, providing a flexible representation of resilience velocity in intricate circumstances. Python pseudocode is in Figure 3.

1. Principal Function
   Hierarchical Particle Filter with Memory and Exogenous Shock

2. Inputs
   a. Observed data (panel structure)
   For each body i=1,…,N, time series: $\{W_{i,t}, D_{i,t}, G_{i,t}, Q_{i,t}, V_{i,t}, P_{i,t}, C_{i,t}\}^{T}_{(t=1)}$
   where $C_{i,t}$, represents the relative resilience response.
   b. Number of particles: $N_p \in [20000,70000]$
   c. Structural dynamic model: $C_{i,t} = S(X_{i,t}, \gamma) + \alpha[C_{i,t-1} - S(X_{i,t-1}, \gamma)] + \beta_i Z_{i,t} + \varepsilon_{i,t}$
   d. Parameter space
   Global parameters: $\gamma=(\gamma_1,\ldots,\gamma_6, \alpha, \beta)$
   with priors: $\gamma \sim N(0,\sigma_\gamma^2)$ and $\alpha \in (-0.95,0.95)$
   Body-specific deviations: $u_i \sim N(0, \sigma_u^2)$
   e. Exogenous shock construction (PCA-based)
      Standardize input variables (G, Q, V, P, W, D)
   Apply PCA
   Retain the first principal component: Zi,t = PCA$_1$(G, Q, V, P, W, D)
   f. Error criterion (robust likelihood)
      Residuals: $\varepsilon_{i,t}=C_{i,t}^{\text{sim}} - C_{i,t}^{\text{obs}}$
      Loss function: $\mathcal{L} = 1/T \sum_t \log(1+\varepsilon_{i,t}^2)$
   g. Particle filter dynamics
      Sequential importance weighting
      Weight update: $wieght_p \propto exp(-\mathcal{L}_p / \sigma_{obs})$
      Effective Sample Size (ESS) monitoring
   Stratified resampling if: ESS < $0.5N_p$
      Adaptive Gaussian jitter for exploration
   h. Hierarchical pooling
      Global parameters shared across bodies
   Idiosyncratic body-level parameters: $\gamma_i = \gamma_{global} + u_i$

3. Outputs
   a. Global parameters estimates: E[γ], Std(γ)
   b. Body-specific exogenous sensitivities: $\beta_i = \beta_{global} + u_{i,\beta}$
   c. Model performance metrics: RMSE, Correlation, ESS trajectories, Parameter uncertainty.
   d. Diagnostic plots

Fig. 3. Pseudocode of the study algorithm. The Python packages used are NumPy, Matplotlib, scikit-learn, and SciPy. They help with numerical computation, visualization, statistical analysis, dimensionality reduction, and probabilistic modeling in the hierarchical particle filtering framework.

Because the hierarchical state-space formulation is not linear and there are hidden components, it is not possible to be sure that all parameters are structurally identifiable. The global structural parameters (γ_1–γ_6), the memory coefficient (α), and the exogenous sensitivities (β_i) all work together to change the latent state, which can cause some parameters to be confused.
To assess practical identifiability, we analyze pairwise correlations between parameters using the empirical distribution obtained from the particle filtering procedure. The resulting correlogram shows that, although moderate correlations exist—reflecting the interconnected nature of the modeled system—there is no evidence of near-perfect linear dependence that would indicate parameter redundancy or lack of distinguishability.

2.2.3. Intra-relationship analysis

Transfer Entropy (TE), as proposed by Schreiber (2000), was employed to examine the interrelationships among variables in the multi-effects supply chain resilience equation. TE is better for looking at time-series data because it shows directionality and dynamic contribution, which correlation methods like Pearson's do not. Pearson's only looks at linear relationships. TE uses probabilities to show how much the past of one variable affects the future of another, showing both directional and nonlinear relationships. It looks at both joint and separate pasts to figure out how strong and where information is flowing. TE is a useful tool for dynamic systems like markets, biological processes, and environmental systems because it can handle nonlinearity, which traditional models can't.

It is important to make clear that this study uses Transfer Entropy as a way to show how information flows between variables in a certain direction, not as a way to measure causal relationships in the strictest sense of the word. TE knows about asymmetric dependencies and dynamic interactions, but it doesn't figure out structural causality on its own or rule out the possibility of hidden confounders. So, the results should be seen as showing that information can be shared and systems depend on each other, not as proof of direct cause-and-effect relationships.

3 Results

For this research, the two most significant disruptions of the last decades were selected as the basis for analysis: the 2008 disruption, which refers to the global financial crisis triggered by the U.S. housing market bubble, and the 2020 disruption, caused by the COVID-19 pandemic, which led to widespread economic and logistics disturbances. Figures 4 and 5 present the relative growth of resilience for the 2008 and 2020 disruptions in Mexico's maritime port system, specifically for the most important Mexican maritime ports (Manzanillo and Lazaro Cardenas). Figure 4 shows two time series of relative growth from 2008 to 2009, with distinct behaviors and cyclical patterns: the left plot displays irregular oscillations around negative values, ending with a sharp drop to about −5.5, indicating a cycle breakdown or shock. The right plot shows clearer, more regular cycles of expansion and contraction, with decreasing amplitude and towards equilibrium. Both series are cyclical but differ in stability: one has collapsing cycles, the other shows damped cycles, suggesting adjustment or convergence.

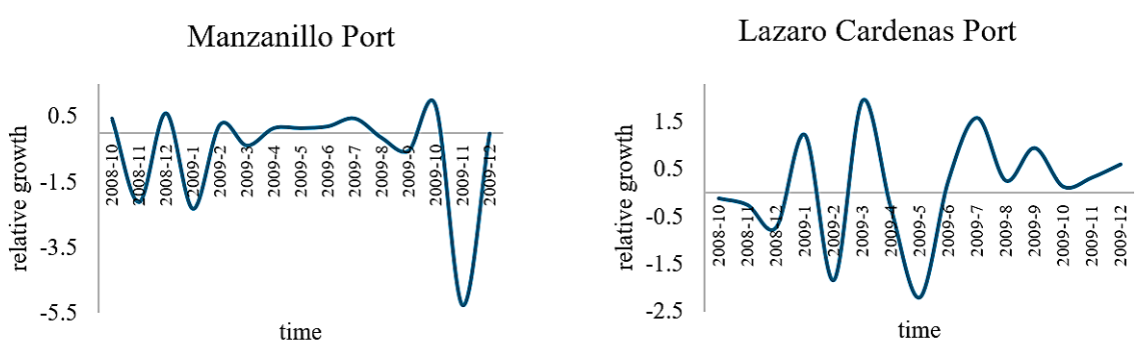

Fig. 4. Resilience Index during the 2008–2009 disruption, showing the results of the proposal resilience measure for the 2008-2009 disruption at the most important Mexican maritime ports (Manzanillo & Lazaro Cardenas), reflecting a highly volatile environment with an underlying cyclical dynamic, albeit with clear differences in stability and resilience.

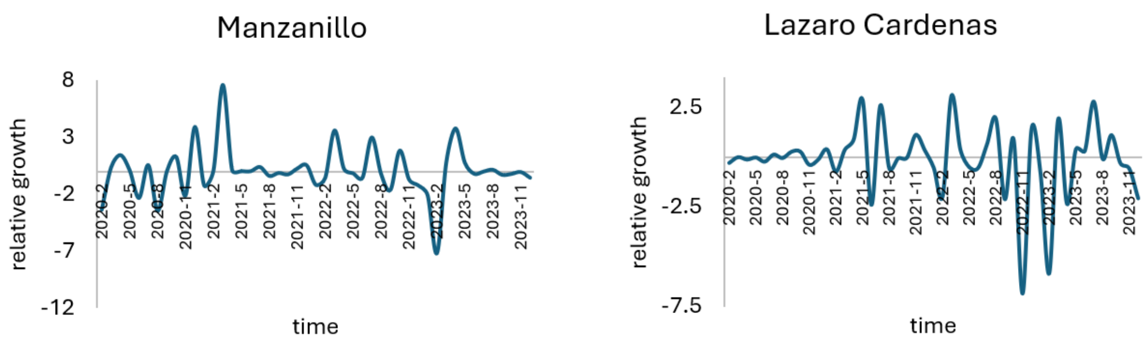

Fig. 5. Resilience Index (2020–2023) during 2020-2023 disruption, showing the results of the proposal resilience measure for the 2020-2023 disruption for the most important Mexican maritime ports (Manzanillo & Lazaro Cardenas ports), reflecting a highly volatile environment with an underlying cyclical dynamic, albeit with clear differences in stability and resilience

Figure 6 illustrates the behavior of the Synchronization effect for both disruptions, showing that the nature of a health-related disruption generates greater disorder across the links in the maritime supply chain, with an upward trend.

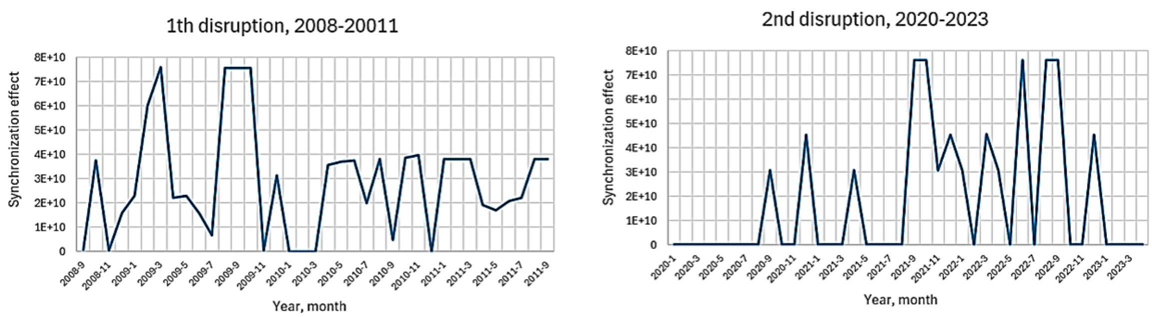

Fig. 6. Synchronization effect. Comparison of resilience Trends During Two Disruptions (2008–2011 and 2020–2023), highlighting fluctuations and long-term recovery patterns with trend lines.

Figure 7 illustrates the behavior of the determinants of the Spillover effect generated in each disruption, showing that the only determinant that exerted a positive external influence during resilience was labor force productivity (L). Specifically, port productivity in Mexico's trade partner countries increased by more than 20% due to Mexican port labor productivity. This result aligns with previous findings on labor force efficiency. A study covering the period from 1982 to 2010, using the Malmquist Index to measure Total Factor Productivity (TFP) in Mexican ports, revealed an average annual productivity growth of 34% (Delfín & Navarro, 2015). In contrast, the behavior of the Spillover effect during a health-related disruption differs significantly.

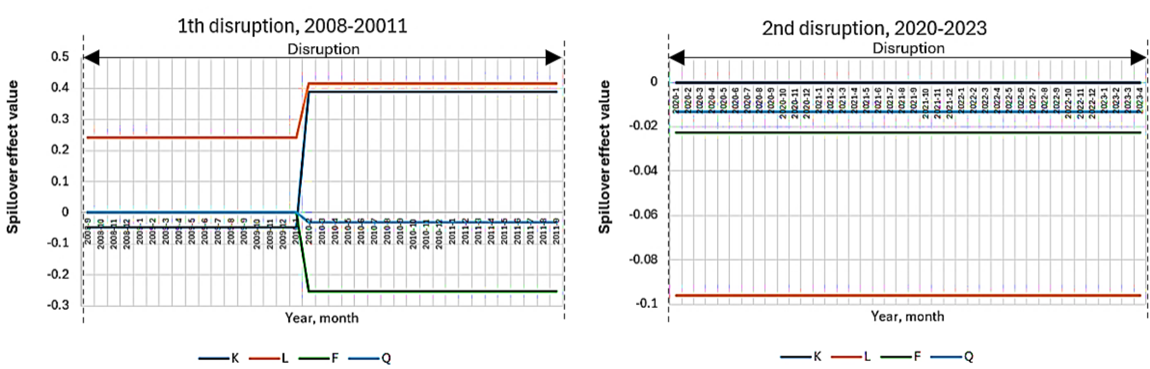

Fig. 7. Spillover effect. Comparison of Spillover Index during two disruptions (2008–2011 and 2020–2023), showing distinct responses across different variables (K: capital stock, L: labor force, F: inflation, Q: intensity in overused assets) over time.

Figure 8 shows that the two studied disruptions behave in a cyclical and different way when it comes to the Bullwhip effect. In both instances, the cyclical characteristic of the Bullwhip effect is apparent, indicating that supply chain participants consistently endeavor to mitigate the impact of demand signals. But there is one important difference: the Bullwhip effect tends to go down during an economic disruption and up during a health-related disruption. This pattern suggests that health-related disruptions impose greater operational damage on supply chains because the quasi-chaotic nature of the efforts required to meet customer demand makes them more prone to disruption.

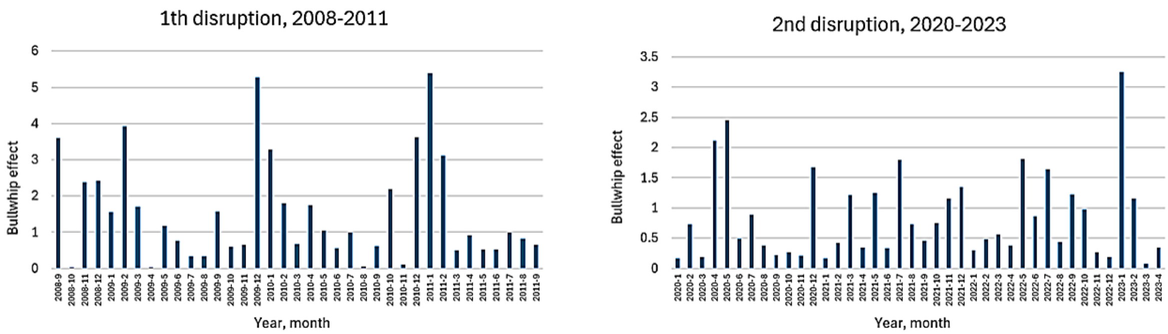

Fig. 8. Bullwhip effect. Comparing changes in the Bullwhip index between the disruptions of 2008–2011 and 2020–2023. The red dotted trend line shows the general direction of each period. The two disruptions show clear differences in their volatility and recovery trends. Figure 8 exhibits recurrent peaks that may resemble seasonal patterns. However, rather than representing purely exogenous seasonality, these fluctuations are interpreted within the framework of this study as endogenous cyclical dynamics associated with the Bullwhip effect and disruption-response mechanisms. Given the structure of the proposed model—which incorporates memory, nonlinear interactions, and external shocks—these patterns are captured as part of the system's intrinsic dynamics rather than treated as separate seasonal components. This perspective is consistent with the objective of analyzing resilience as a dynamic multi-effect process rather than as a purely periodic phenomenon.

Figure 9 highlights differences in economic and health disruptions, showing Ripple effects; they increased during the 2008 crisis but decreased in 2020. This indicates Mexico's maritime supply chains used ineffective strategies in 2008, leading to worsening disruptions and operational instability as the crisis continued.

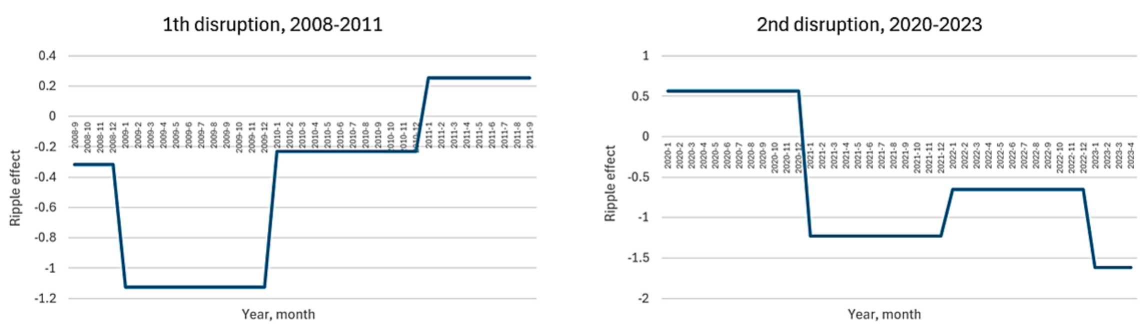

Figure 9. Ripple Effect. Comparison of Ripple effect index trends during 2008–2011 and 2020–2023 disruptions. The red dotted line shows an initial upward trend followed by a downward trend, highlighting distinct resilience patterns and long-term impacts.

Figure 10 shows that the economic effects during the resilience periods of the studied disruptions are both going down, with a bigger drop during the health-related disruption. Economic growth was more affected by the 2020 pandemic than the 2008 crisis. Inflation rose about 12% during both resilience periods. Labor force growth, however, was only 1.82% during health disruptions versus 13.33% during economic disruptions. This highlights the importance of capital and labor in supply chain resilience and economic recovery.

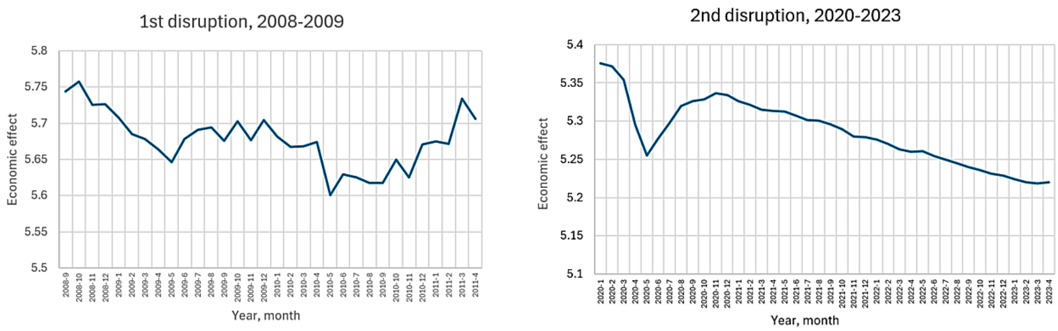

Fig. 10. Economic effect. Analysis of economic impact index developments throughout the interruptions of 2008–2009 and 2020–2023. The red dotted trend lines signify a gradual decrease in both intervals. Notwithstanding variations, the general decline indicates a sustained effect on resilience.

As illustrated in Figure 11, preventive action in the supply chain emphasizes the multiplier effect of the port sector. Resilience means having programs in place to stop problems before they happen. In Mexico, when people are more confident, they don't spend as much on risk prevention because they don't think the risk is as high. The inverse index (INEGI, 2024) shows that investments in risk prevention go up when confidence starts to fall. Investments in risk prevention went down during economic problems but up during health problems, showing that people reacted differently.

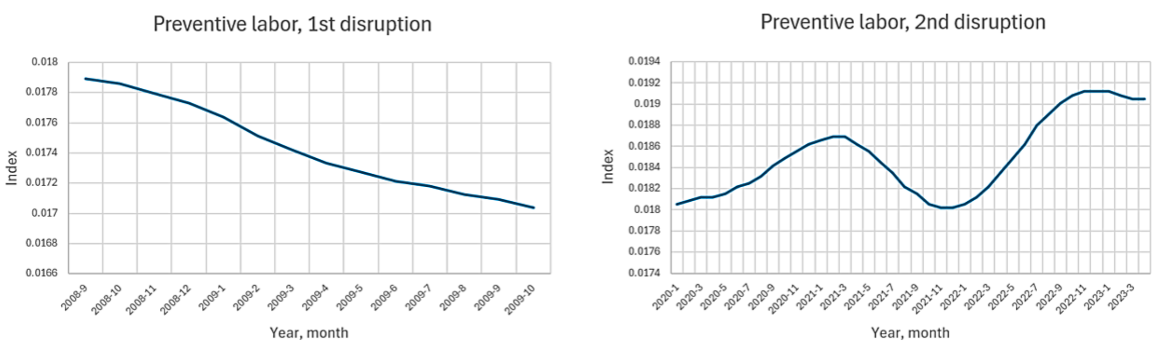

Fig. 11. Preventive labor. A look at how preventive labor trends changed between the first and second disruptions. The first disruption shows a steady drop, while the second shows cyclical changes with a rise. The red dotted trend lines show how the long-term paths in each period are different.

Figure 12 reveals a distinctive pattern: although the studied variables have thus far exhibited unfavorable and aggressive behavior in response to the health-related disruption, the tonnage received and handled within Mexico's maritime port system was higher during the pandemic.

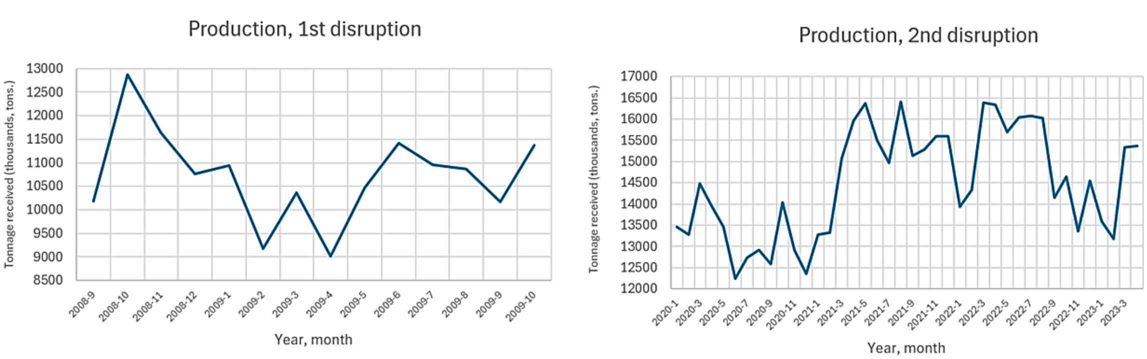

Fig. 12. Behavior of Maritime Port Production. A look at how production changed during the first and second disruptions. The first disruption shows a drop, then some ups and downs, while the second shows a rise. The red dotted lines show how the recovery patterns are different.

The algorithm in Figure 3 uses the variables from [1] to give estimates of parameters, tests of significance, and measures of reliability (Figures 13 and 14). This evaluates the behavior, stability, and inferential capabilities of the hierarchical particle filtering model. Adding global variances keeps particle diversity and stops filter collapse. The prediction errors have a multi-stage structure, and medium- and long-term trajectories are preserved, while short-term oscillations are smoothed. Probabilistic forecasts with confidence intervals show that uncertainty is mostly bounded and makes sense. Scatter diagrams show the internal consistency structure more than the fact that the predicted values are very close together. So, confirmation through the convergence of parameters and their sensitivities to external contributions would make memory effects and external effects on resilience stand out more. Figures 13 and 14 summarize the model's estimation performance and diagnostic properties. For clarity, each subpanel is described separately:

Model diagnostics and estimation performance, Particle filter provides reliable estimates of resilience from 2008 to 2009 (see Figure 13), in which each subpanel highlights key aspects of the model's performance under the baseline specification:

(a) Particle variance of global parameters
The posterior variance of global parameters stays within reasonable and manageable limits.
This shows that the estimation process is well-balanced and stable.
The dispersion observed across parameters reflects appropriate model flexibility rather than estimation noise.
(b) Robust prediction error across bodies
Most units have low and stable prediction errors.
This means that the model fits well across different types of cross-sectional observations.
The limited presence of higher-error units highlights the model's robustness in diverse conditions.
(c) Observed vs estimated resilience velocity
The estimated series closely follows the overall trends in the data that was observed.
The model does a good job of showing short-term changes in a smooth way while also capturing long-term trends.
This behavior is in line with a strong filtering method that puts structural signal ahead of noise.
(d) Prediction with credibility interval (Body 0)
The 90% credibility interval successfully includes most of the values that were seen.
This shows that the uncertainty quantification is accurate and the probabilistic predictions are well-calibrated.
Changes in the width of the interval accurately show how the system's uncertainty changes over time.
(e) Convergence of global parameters
The posterior distributions show a clear unimodal pattern.
This shows that the estimation algorithm is converging steadily.
The distributions are relatively concentrated, which means that finding the right parameters should be easy.
(f) Distribution of body-specific exogenous effects
The distribution of β_i reveals meaningful heterogeneity across units.
The even spread around the central tendency shows that there is no systematic bias in exogenous sensitivity.
This backs up the model's ability to show how different things are in a clear way.

Model diagnostics and estimation performance, Particle filter provides reliable estimates of resilience from 2020 to 2023 (see Figure 14), in which this figure presents the model's behaviour under a more demanding or extended setting:

(a) Particle variance of global parameters
Parameter variances remain well-controlled despite the increased complexity of the dataset.
This reflects the robustness of the estimation framework under more demanding conditions.
The consistency with Figure 13 supports the stability of the model structure.
(b) Robust prediction error across bodies
Although variability increases slightly, prediction errors remain within acceptable ranges.
The model maintains a satisfactory level of predictive performance across units.
This demonstrates resilience of the estimation approach under more heterogeneous conditions.
(c) Observed vs estimated resilience velocity
The estimated series continues to capture the main dynamics of the observed process.
The model can still find structural patterns even when there is more variability.
This shows that the framework can handle more complicated time-based behaviors.
(d) Prediction with credibility interval (Body 0)
Credibility intervals expand in periods of higher variability, reflecting appropriate uncertainty adaptation.
Most observed values remain within the predicted bounds.

This shows that the model can still make accurate probabilistic predictions even when things are less stable.

(e) Convergence of global parameters

Posterior distributions remain well-defined and centered.

Slightly increased dispersion is consistent with the added complexity of the scenario.

Overall, convergence remains stable and satisfactory.

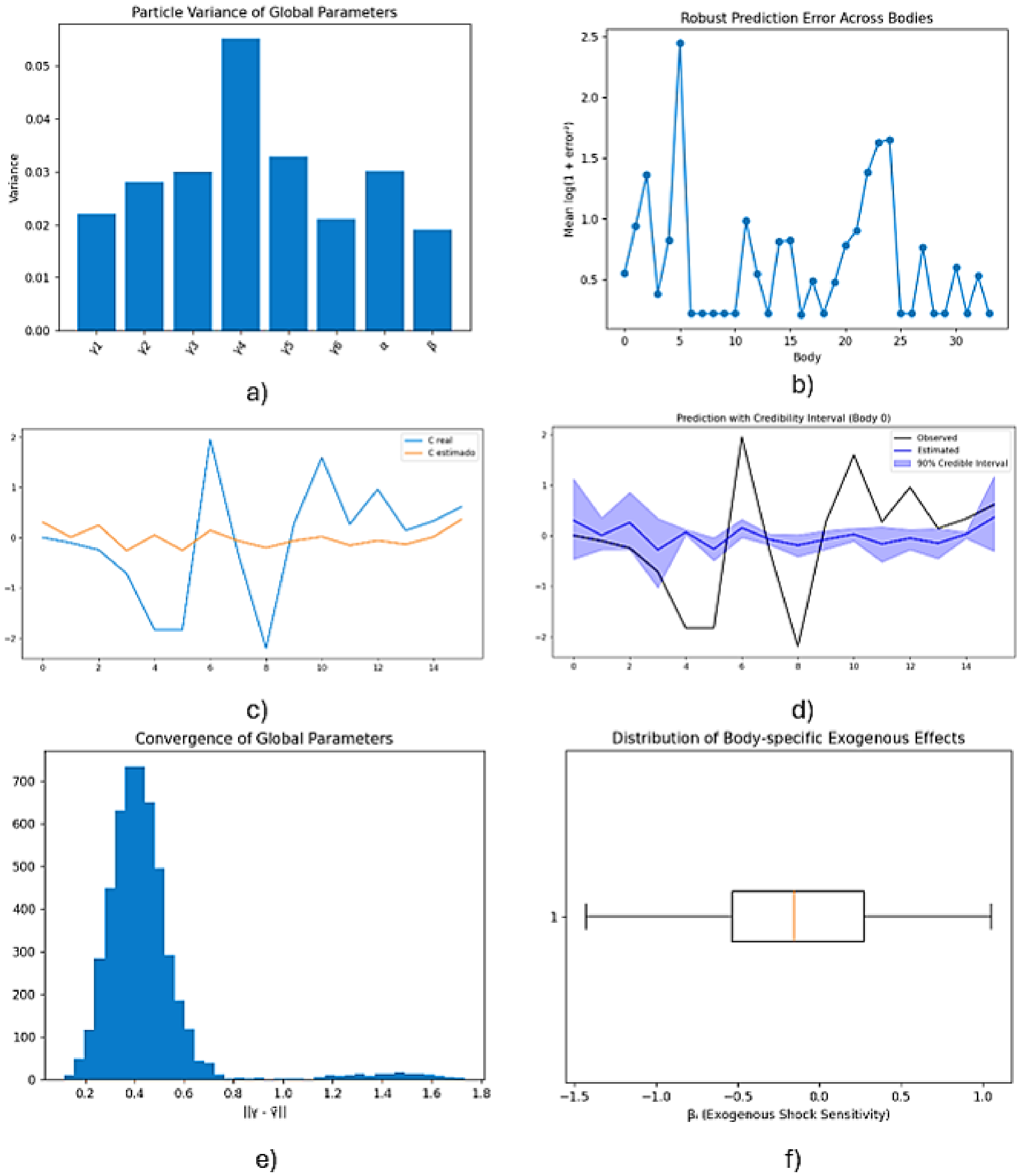

Fig. 13 The text shows that the Particle filter provides reliable estimates of resilience from 2008 to 2009, giving consistent and accurate results for a number of different parameters. The global parameters (γ_1–γ_6, α, β) change at the last iteration, but they are not zero and are limited, which means that the particles are highly diverse and that the process can converge. b) The mean log-squared residuals, which show prediction errors, are different for each entity. This shows how the model is set up in a hierarchy and how it reacts to changes. The resilience dynamics for Body 0 show how structural features affect trajectories by capturing medium-term trends and smoothing out high-frequency changes. d) The comparison of the observed and expected resilience for Body 0 within a 90% credibility range shows that most of the predictions are still within the limits that have been set. e) The last distribution of global parameters is unimodal and focused, which means that the filter has converged and the estimates are reliable. f) The exogenous shock coefficients (β_i) differ between bodies, showing that they are exposed to different amounts of external shocks.

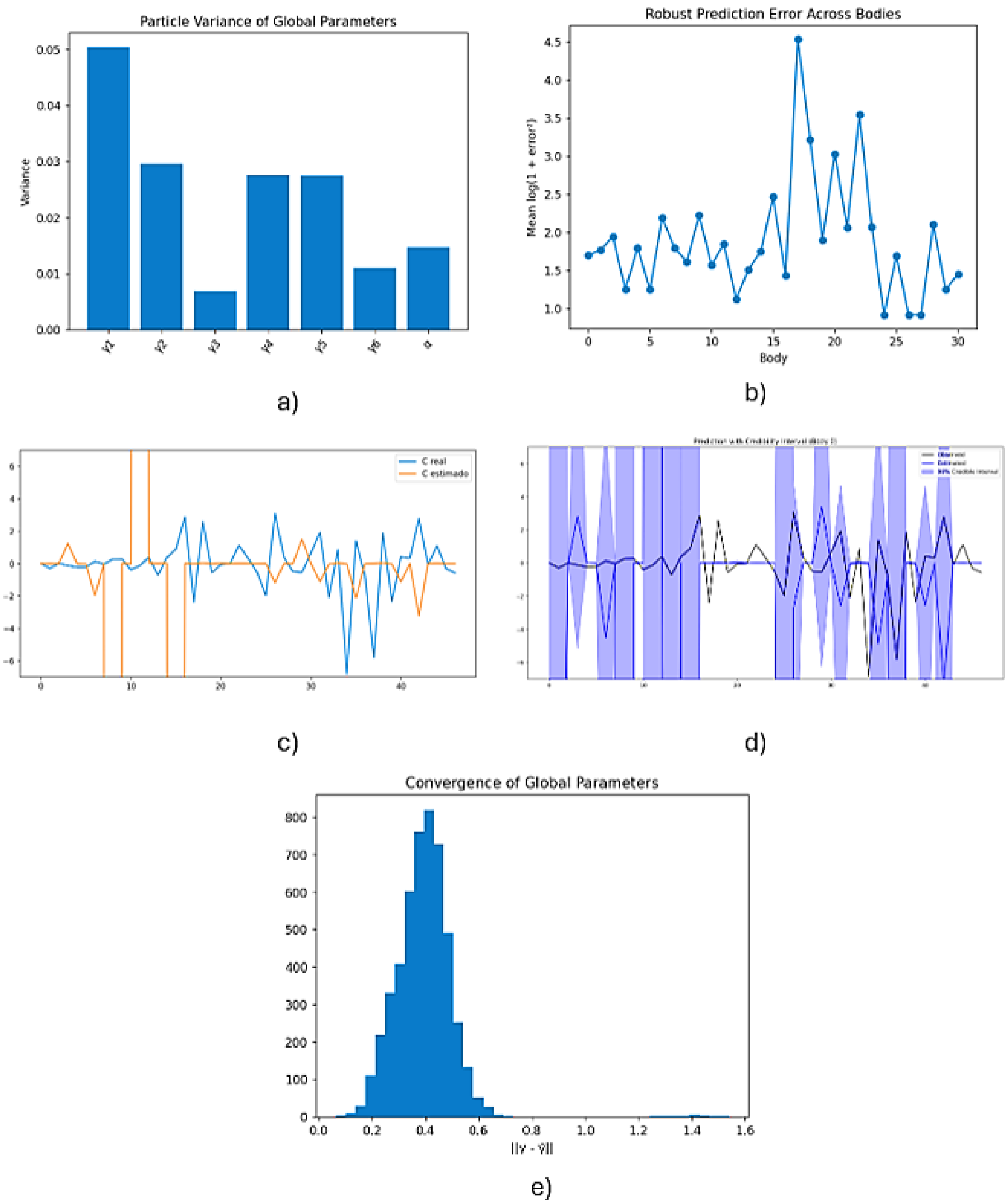

Fig. 14. The Particle filter for resilience (2020–2023) consistently produces correct results. The differences in the estimated parameters (γ_1–γ_6, α) show that there is enough variety and no signs of degeneration, which supports both stability and convergence. Variance shows how uncertain structural and memory parameters are during shocks and times when memory isn't very good. The mean log-squared residuals show how much prediction error changes across 30 bodies. The differences show where dynamics differ from the overall trend. The observed versus estimated dynamics for Body 0 show how global parameters and limited memory affect it ($\alpha \approx -0.47$). Short-term changes are smoothed out, and medium-term trends are well captured. The 90% credibility interval for Body 0's forecast shows that most observations are within the bounds, even though there are some fluctuations due to memory effects. This suggests that the calibration is good. The last estimates of the parameters are unimodal and concentrated, which shows that they have converged and are stable. The dynamics are mostly caused by immediate effects and weak negative memory.

Even though the model has a nonlinear and hierarchical structure, parameter identifiability is made possible by the different structural roles that each group of parameters plays in the state dynamics. The coefficients γ_1–γ_6 control how the latent process spreads over time, and they are different for each lag. The global parameter α, on the other hand, measures overall memory and controls the system's overall memory. On the other hand, the body-specific coefficients β_i only come in through the exogenous shock component, which adds cross-sectional heterogeneity that is not related to the endogenous temporal dynamics. This classification of temporal, global, and cross-sectional channels limits the possibility of functional substitution among parameters and diminishes the probability of confounding variables. The empirical results show that the posterior distributions are stable and unimodal, and that the particle filtering process always comes to a conclusion. This suggests that the model does not allow for multiple parameter combinations that give the same likelihood contributions. These traits show that something can be identified in a practical way, even when there are hidden states and nonlinearities. The results were also found to be qualitatively strong when different prior specifications were used. This means that the parameter estimates are stable and not very sensitive to prior assumptions.

Subsequently, the Transfer Entropy technique was applied to determine the direction of information flow between the independent variables. The results are as follows: As illustrated in Figure 15, the Bullwhip effect demonstrates a significant transfer of information to both International Reserves (0.6206) and Public Spending (0.6667) in this direction. Additionally, a high bidirectional information transfer is observed between the variables International Reserves and Public Spending. This indicates that the Bullwhip effect exhibit significant directional information transfer toward International Reserves and Public Spending during the economic disruption of the 2008 crisis.

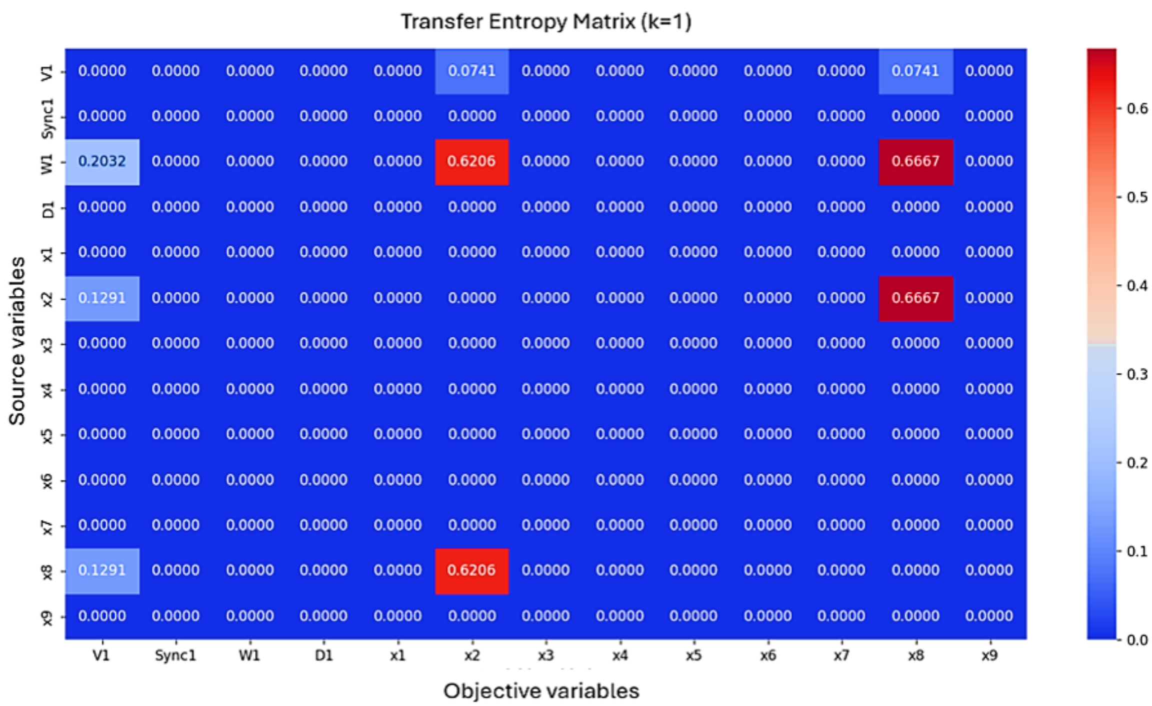

Fig. 15. Transfer Entropy Matrix for Period 2008-2010. V1= Spillover effect; Sync1= Synchronization effect; W1: Bullwhip effect; D1= Ripple Effect; x1=exchange rate; x2= International reserves; x3=Inflation rate; x4=Credit cost; x5=GDP (Gross domestic product); x6=FDI (Foreign direct investment); x7=unemployment rate; x8=Public spending; x9= Current account; x9=Broad money (M3).

Subsequently, as shown in Figure 16, during the stable period (2011–2019), the same behavior described previously is observed, albeit with greater intensity. Additionally, the Bullwhip effect is a significant predictor of the Ripple effect. This Ripple effect also exhibits significant directional information transfer for the same variables, International Reserves and Public Spending.

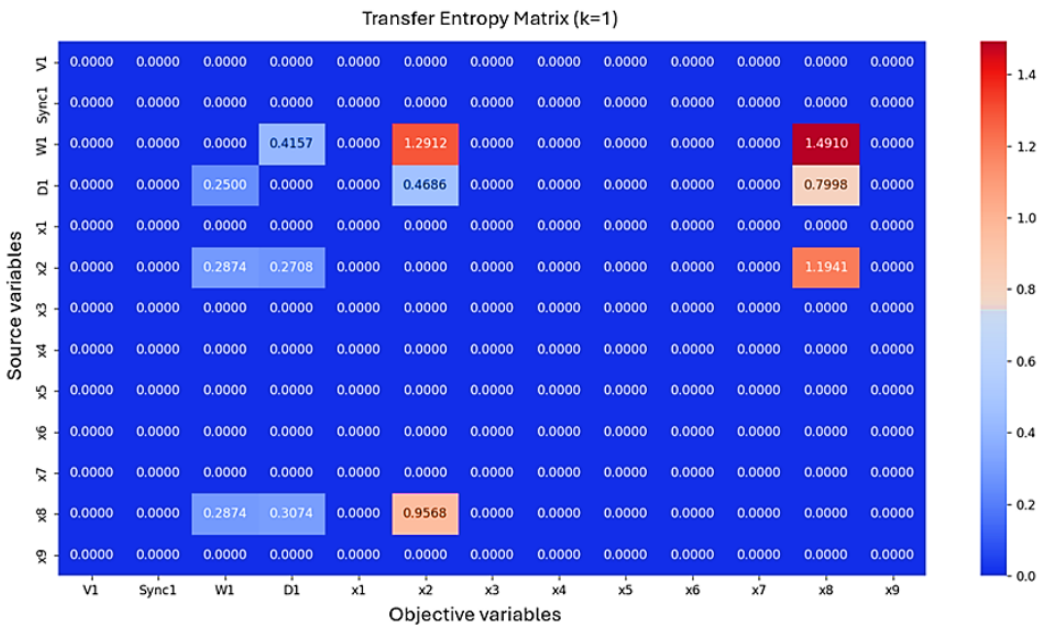

Fig. 16. Transfer Entropy Matrix for Period 2011-2019. V1= Spillover effect; Sync1= Synchronization effect; W1: Bullwhip effect; D1= Ripple Effect; x1=exchange rate; x2= International reserves; x3=Inflation rate; x4=Credit cost; x5=GDP (Gross domestic product); x6=FDI (Foreign direct investment); x7=unemployment rate; x8=Public spending; x9= Current account; x9=Broad money (M3).

Finally, as shown in Figure 17 (period 2011–2019), the same transfer pattern observed during the economic disruption of 2008 is again evident. Specifically, the Bullwhip effect shows significant directional information transfer toward the variables International Reserves and Public Spending, and a bidirectional predictive relationship between them.

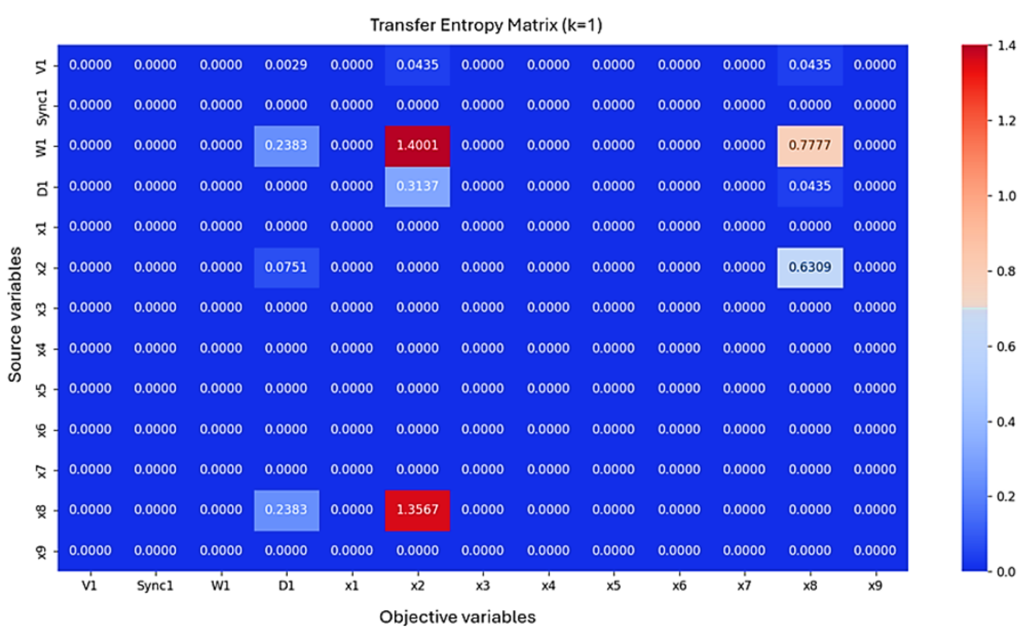

Fig. 17. Transfer Entropy Matrix for Period 2020-2023. V1= Spillover effect; Sync1= Synchronization effect; W1: Bullwhip effect; D1= Ripple Effect; x1=exchange rate; x2= International reserves; x3=Inflation rate; x4=Credit cost; x5=GDP (Gross domestic product); x6=FDI (Foreign direct investment); x7=unemployment rate; x8=Public spending; x9= Current account; x9=Broad money (M3).

The results show that government spending and international reserves can contribute to changes in demand by affecting the stability of the economy and people's trust in it. Reserves act as a financial buffer; declines may prompt changes in consumer spending, shifting demand unrelated to market factors. Government spending also influences demand: increases can signal economic stimulus, stimulating consumption, while reductions may indicate fiscal tightening or recession.

Resilience stage 1st Disruption 2008-2009	Synchronization (α_{Φ})	Spillover (α_{Λ})	Bullwhip α_{W})	Ripple (α_{D})	Economics (ratio)	Production (α_{Γ})	Preventive Labor (α_{φ})
Resilience velocity (S)	0.2425	-0.1193	-0.2112	-0.5336	4.8773	0.3472	-0.5978
α(memoria): mean=-0.4277, std=0.1736 β(exógeno): mean=0.1159, std=0.1379 RMSE Lazaro Cardenas Port: 1.058867 Corr (S_obs, S_est): 0.4151							

Fig. 18. Resilience behavior (S), 2008-2009 disruption

Resilience stage 2nd Disruption 2020-2023	Synchronization (α_{Φ})	Spillover (α_{Λ})	Bullwhip α_{W})	Ripple (α_{D})	Economics (ratio)	Production (α_{Γ})	Preventive Labor (α_{φ})
Resilience velocity (S)	0.4350	-0.1745	0.8425	0.6697	5.0090	0.0090	0.3958
α(memoria): mean=-0.4689, std=0.1212 RMSE Lazaro Cardenas Port: 46.283187 Corr (S_obs, S_est): 0.0724							

Fig. 19. Resilience behavior (S), 2020-2023 disruption

Figures 18 and 19, shows a comprehensive visualization of the parametric results obtained through the proposed algorithm, illustrating the resilience associated with various types of disruptions examined in this study (Synchronization, Spillover, Bullwhip, Ripple, economic effects). These figures detail how the system will respond to different disruptions, highlighting important patterns (arrows) and variability in resilience dynamics.

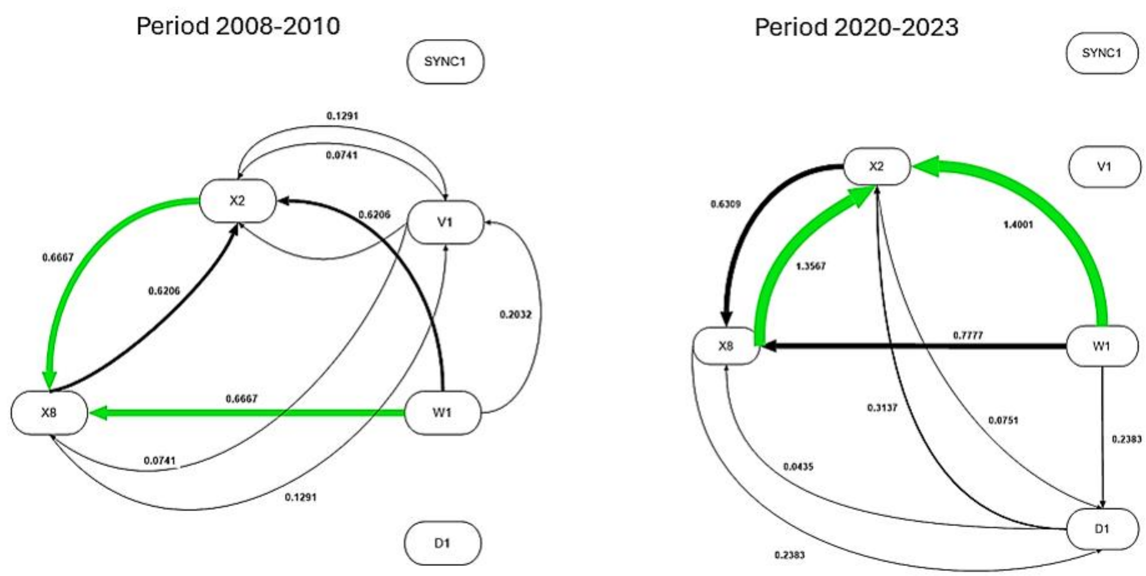

Fig. 20. Directed interaction networks between resilience effects and macroeconomic indicators across three disruption periods. Networks depict significant interactions (derived from Transfer Entropy analysis) between resilience effects (Sync1: Synchronization, V1: Spillover, W1: Bullwhip, D1: Ripple, Econ: Economic ratio) and selected macroeconomic indicators (e.g., x2: International reserves, x8: Public spending). Arrows indicate the direction of significant directional information (source → target), edge green represents the strongest contribution, and edge thickness is proportional to normalized TE values. At the same time, the behavior of resilience velocity for each effect under study is shown across the different resilience stages in Figures 18 and 19.

3.1. Discussion and implications of the results

The integrated findings from Transfer Entropy (Figures 15–17) and parametric resilience analysis (Figures 18,19) elucidate the interplay of various logistic effects with macroeconomic indicators and the progression of their quantitative impacts on resilience velocity throughout disruption phases. The arrow thickness in Figure 20 identifies high-intensity contribution channels, and Figures 18–19 illustrate the directional impact (positive or negative) of each effect at each resilience stage.

General statistic overview for 2008-2009 study period: During this period, a correlation of 0.4151 was identified, indicating that the proposed model captures the temporal direction acceptably, since the series represents relative changes. Furthermore, the result is fully robust, as the model is not designed for forecasting but rather for representing the system's natural structural behavior. The system’s memory (α=-0.4277) indicates that past adjustments of the system exhibit a moderate inverse strength. The exogenous factor (β=0.1159), clearly different from zero and of moderate magnitude, providing evidence of a common exogenous factor not explained by the logistic effects under study that drives resilience. Within this exogenous effect, the sensitivity of the maritime ports under analysis was identified. The most important ports are classified into three groups (in that order of importance, from highest to lowest), which confirms that this exogenous shock is not uniform, as some ports transmit it, others dampen it, and others react in the opposite direction:

a) Maritime ports highly sensitive to exogenous economic effects: Puerto of Acapulco, Puerto of Pichilingue, Puerto of Salinas Cruz, Puerto of Ensenada.
b) Maritime ports practically immune to exogenous economic effects: Port of Coatzacoalcos, Port of Chiapas, Port of Manzanillo.
c) Maritime ports that react in the opposite direction to the exogenous effect: Port of Morelos, Port of Isla San Marcos, Port of Isla de Cedros.

General statistical overview for the 2020–2023 study period: During this period, a low correlation of 0.0724 was identified, indicating that the proposed model continues to capture the temporal direction acceptably, given that the series represents relative changes. Moreover, the result is fully acceptable, as the model is not designed for forecasting but rather for representing the system's natural structural behavior. The system’s memory (alpha = -0.4689) indicates that past adjustments to the system exhibit a moderate inverse strength. For this study period, the exogenous factor was removed (β) because this element renders the results of the proposed model statistically insignificant, indicating that, for this period, such a shock is irrelevant, as it is already embedded throughout the entire study period through the effect of COVID-19 itself and its intrinsic nature as a shock.

3.1.1 Bullwhip Effect as a Driver of Public Spending

Statistical interpretation:
In the 2008–2009 disruption, the thickest edges in Figure 20 are W1 → x8 (TE = 0.6667) and x2 → x8 (TE from reserves to spending), indicating strong fiscal responsiveness to both operational variability and reserve status. Parametric data from Figure 18 show that during this period, the Bullwhip effect had a negative coefficient on resilience (-0.2112), meaning that it consistently acted as a drag on resilience. The fact that the Bullwhip effect still positively contributed Public Spending (x8) in the TE network (0.6667) suggests that fiscal expansion was used to counteract this operational drag. Additionally, it influenced international reserves (0.6206), indicating that in this type of crisis, exports tended to accumulate international reserves due to high export inflows and competitive external prices. The Bullwhip effect also had a positive effect on Spillover (0.2032), which means that the good situation created by those low prices spread throughout the system.

During the 2020–2023 pandemic, Bullwhip coefficients turned positive (0.8425), indicating that increased demand signal amplification contributed to the construction of safety stocks in warehouses and to redundancy through supplier diversification. Moreover, the Bullwhip effect appears to have provided appropriate alarm signals at various points of uncertainty throughout COVID-19, generating new knowledge to understand unfamiliar protocols within supply chain dynamics under pandemic disruption. Figure 20 shows that its links to public spending (x8) and international reserves (x2) act in a way that is similar to the first disruption. The only difference is that the intensity is higher for international reserves than for public spending. The effect on Spillover is zero, but the positive effect (0.2383) on the Ripple effect shows that during the pandemic, operational mistakes and shocks were made worse, which caused earlier, worse bottlenecks and more volatility.

Managerial implication:
During crises, authorities should use Bullwhip metrics as early warnings to control spending and make demand less variable. When there is a health crisis, managers should work to stop the Bullwhip effect from having bad effects, especially the volatility it causes.

3.1.2. Role of Spillover Effect in Disruption Networks

Statistical interpretation:
From 2008 to 2009, the Spillover variable (V1) responded marginally but positively to X8 and X2. From a parametric point of view, negative contributions were seen in resilience (-0.1193), which means that the maritime port system produced negative results for its outside partners. These effects showed up as errors spreading, productivity problems, and problems with transferring technology and knowledge. A similar pattern is observed during the 2020–2023 period.

Managerial implications:
The Spillover effect is a big chance for both types of disruption because it has a bad effect in both cases. During a pandemic crisis, managers should pay more attention to it. This is especially important because resilience has a stronger negative effect (-0.1745). Digital resource sharing, artificial intelligence, big data, and technology transfer mechanisms are all operational channels that should be given special attention because they are limited by mobility and capacity. During pandemic crises, a more proactive approach to soft skills is required, as Spillover effects tend to operate less visibly within daily operations. We observed that the Spillover effect was the only effect that negatively affected both disruptions.

3.1.3. Synchronization Effect as a source of double levering in pandemics

Statistical interpretation:
In 2008–2009, Synchronization coefficients were positive in all types of crises (0.2425 and 0.4350), indicating that they consistently support resilience. Besides, it has almost double the force on the pandemic disruption type. We observe that the Synchronization effect is the unique effect that positively leverages resilience. Figure 20 confirms that, regardless of the type of disruption, the synchronization effect remains neutral with respect to contribution effects, whether logistics or economic. It means that the Synchronization effect is cleaner, pivoting on resilience, and shows a high level of independence from the other variables.

Managerial implication:

Sustaining Synchronization throughout resilience is critical, especially amid pandemic disruptions. Managers must have real-time operational technologies linked to economic indicators to help identify when Synchronization failures risk harming resilience and stability. This issue also means that, the Synchronization effect is particularly more effective in pandemic disruptions because they spread rapidly, non-linearly, and across multiple levels at once, causing any lack of coordination in timing, information, or actions to amplify disorder; Synchronization brings actors' decision-making into line, lowers social entropy, stops strategic dissonance, allows collective learning, and lets human responses better match the pace of the biological phenomenon. This restores systemic coherence and gives people more control, even when there is a lot of uncertainty. Because those results are so important, the manager should stop being a resource optimizer and start being a Synchronization orchestrator. This person is in charge of making sure that people, information, and decisions are all in sync so that the company can respond as a single system when things go wrong. From these findings, we can infer that health-related disruptions require a higher degree of coordination and cooperation among supply chain links compared to economic disruptions. At the same time, however, these disruptions may also reduce the system's effective capacity for synchronization, as workforce shortages due to illness and restrictive measures limit operational responsiveness. This dual effect helps explain the more pronounced instability and coordination challenges observed under health-related shocks.

3.1.4. Ripple Effect predictability and its role in pandemics

Statistical interpretation:
From 2008 to 2009, Ripple coefficients were negative for economic disruption (−0.5336), whereas those for pandemic disruption were positive (0.6697). These results suggest that bottleneck velocity was intensified during the economic disruption. However, it occurs the contrary way on pandemic one: The domino effect is not intrinsically negative in disruptive scenarios, as it is context-dependent and its impact depends on what is propagated, when it is propagated, and the level of Synchronization; although it is often harmful when it amplifies errors, bottlenecks, or misinformation, it can become beneficial when it accelerates the adoption of clear and simple decisions, reinforces coherence and collective trust, breaks the inertia of paralyzed systems, and—especially in chaotic moments where life or system survival depends more on speed than on precision—becomes a key factor in initiating recovery and restoring responsiveness. In 2008–2009 (Figure 16), the Ripple effect had no contribution, unlike the pandemic disruption, due to the aforementioned cause.

Managerial implication:
This means that when things go wrong, managers need to remember what their jobs are and that they need to make tools for each situation, not just avoid them. This means knowing when to start a good domino effect on purpose—by making choices simple, rules clear, and actions clear—to speed things up and break the paralysis, and when to stop it to keep mistakes from getting worse once the system is stable. It also involves managing timing, putting speed ahead of accuracy during times of chaos, and then moving on to refinement and control. In the end, managers need to be architects of coherence. They need to carefully control the signals they send, how those signals spread through the organization, and how far they should go. This is because in disruptive situations, leadership is less about making the best decision on its own and more about making sure the system can respond in a timely and aligned way.

This study focuses on the Mexican maritime port system; however, the suggested resilience velocity model—featuring Synchronization, Spillover, Bullwhip, Ripple, and economic effects—can be modified for application in various industries, regions, and disruption types. Its structure is not based on any one sector, and it needs similar operational, structural, and economic indicators. For example, in manufacturing, synchronization has to do with the balance between production and inventory, spillover has to do with transferring capacity, and ripple has to do with supplier dependencies. In energy networks, errors in predicting demand can cause Bullwhip effects, and grid balancing can cause Synchronization.

The suggested framework is meant to be structurally transferable between sectors because it doesn't depend on functional forms that are specific to one sector. Instead, it is based on general ideas about nonlinear dynamic interactions, memory effects, and exogenous perturbations. But this transferability only works in some situations. In particular, the target system must have (i) state variables that can be measured and change over time, (ii) interaction mechanisms that can be shown through nonlinear dynamics, and (iii) sensitivity to shocks or changes from outside sources.

In these situations, the model parameters (γ, α, β_i) can be given new meanings to show how things work in different sectors, while still keeping the basic structure of the framework. Because of this, the model should be seen as structurally generalizable but parametrically adaptable, not as something that can be used without recalibration in all situations.

The model's particle filtering and machine learning can deal with different kinds of problems, like natural disasters, geopolitical shocks, and pandemics, by changing parameters and data. Its adaptive design, which changes based on the stage, lets you make meaningful comparisons between sectors and regions by treating resilience as a changing quantity instead of a fixed one.

4 Conclusions

This study investigates five effects—Synchronization, Spillover, Bullwhip, Ripple, and economic factors—on supply chain resilience within the Mexican port system during the 2008–2009 crisis and the 2020–2023 COVID-19 pandemic. It uses a nonlinear model, hierarchical particle filtering, and TE network analysis to measure the effects of each effect and connect them to resilience. The model figures out hidden shocks and gets resilience velocity from changes in the system, taking into account feedback and outside shocks. Hierarchical filtering with strong weighting is used to figure out the parameters. The results indicate that from 2008 to 2009, the Bullwhip effect was associated with public expenditure, adversely impacted resilience, and favorably affected reserves and Spillovers. Bullwhip was very good from 2020 to 2023 because it helped build up inventory, diversify, and learn. There were fewer spillovers and more ripple effects, which made things more unstable. Spillover effects were good for public spending and reserves, but they hurt resilience, especially during pandemics. To lessen the bad effects, managers should focus on digital tools, soft skills, and policies that are proactive. During pandemics, synchronization always made resilience stronger by making sure that operations and information were in sync. There was a different Ripple effect in each case. Resilience hurt when the economy was bad, but it helped during pandemics by making decisions quickly. The framework is adaptable beyond ports to other infrastructures. Overall, resilience depends on the strength and placement of effects within macroeconomic networks, requiring balanced quantitative and topological strategies.

Conflicts of Interest

The author(s) does/do not have any type of conflict of interest to declare.

Data Availability

All data used in this study is available from the corresponding author upon request.

Funding

The authors did not receive any sponsorship to carry out the research reported in the present manuscript.

References

Acosta Terán, M. (2023, February 27). *Guía básica del arrastre de contenedores desde/hacia Altamira, Veracruz y Manzanillo*. Mexicom Logistics. https://mexicomlogistics.com/es/arrastre-contenedores-altamira-veracruz-manzanillo-2/

Al-Hourani, S., & Weraikat, D. (2025). A systematic review of artificial intelligence (AI) and machine learning (ML) in pharmaceutical supply chain (PSC) resilience: Current trends and future directions. *Sustainability, 17*(14), Article 6591. https://doi.org/10.3390/su17146591

Bathke, H., Münch, C., von der Gracht, H. A., & Hartmann, E. (2024). Building resilience through foresight: The case of maritime container shipping firms. *IEEE Transactions on Engineering Management, 71*, 10534–10556. https://doi.org/10.1109/TEM.2021.3137009

Behera, A. K., & Ramanathan, K. (2022). An effective disaster recovery model in supply chain management at times of pandemic. *Cardiometry*, (25), 502–510. https://doi.org/10.18137/cardiometry.2022.25.502510

Browning, T., Kumar, M., Sanders, N., Sodhi, M. S., Thürer, M., & Tortorella, G. L. (2023). From supply chain risk to system-wide disruptions: Research opportunities in forecasting, risk management and product design. *International Journal of Operations & Production Management, 43*(12), 1841–1858. https://doi.org/10.1108/IJOPM-09-2022-0573

Cavalcante, I. M., Frazzon, E. M., Forcellini, F. A., & Ivanov, D. (2019). A supervised machine learning approach to data-driven simulation of resilient supplier selection in digital manufacturing. *International Journal of Information Management, 49*, 86–97. https://doi.org/10.1016/j.ijinfomgt.2019.03.004

Cavallo, A., & Rigobon, R. (2016). *The Billion Prices Project: Using online prices for measurement and research* (NBER Working Paper No. 22111). National Bureau of Economic Research. https://doi.org/10.3386/w22111

Chowdhury, M. M. H., & Quaddus, M. A. (2015). A multiple objective optimization based QFD approach for efficient resilient strategies to mitigate supply chain vulnerabilities: The case of garment industry of Bangladesh. *Omega, 57*, 5–21. https://doi.org/10.1016/j.omega.2015.05.016

Chowdhury, P., Paul, S. K., Kaisar, S., & Moktadir, M. A. (2021). COVID-19 pandemic related supply chain studies: A systematic review. *Transportation Research Part E: Logistics and Transportation Review, 148*, Article 102271. https://doi.org/10.1016/j.tre.2021.102271

Christopher, M., & Peck, H. (2004). Building the resilient supply chain. *The International Journal of Logistics Management, 15*(2), 1–14. https://doi.org/10.1108/09574090410700275

Chukwuka, O. J., Ren, J., Wang, J., & Paraskevadakis, D. (2023). A comprehensive research on analysing risk factors in emergency supply chains. *Journal of Humanitarian Logistics and Supply Chain Management, 13*(3), 249–292. https://doi.org/10.1108/JHLSCM-10-2022-0108

Coordinación General de Puertos y Marina Mercante. (2026). *Estadística mensual acumulada de los puertos de México 2026*. Retrieved 1 August 2026, from https://www.gob.mx/puertosymarinamercante/acciones-y-programas/estadistica-mensual-acumulada-de-los-puertos-de-mexico-2026

Creswell, J. W. (2014). *Research design: Qualitative, quantitative, and mixed methods approaches* (4th ed.). SAGE.

Delfín Ortega, O. V., & Navarro Chávez, J. C. L. (2015). Productividad total de los factores en las terminales de contenedores en los puertos de México: Una medición a través del índice Malmquist. *Contaduría y Administración, 60*(3), 663–685. https://doi.org/10.1016/j.cya.2015.05.011

Denzin, N. K., Lincoln, Y. S., Giardina, M. D., & Cannella, G. S. (Eds.). (2024). *The SAGE handbook of qualitative research* (6th ed.). SAGE.

Dessouky, M. (2020). *Efficient empty container movement considering the next day's demand can reduce port congestion* [Research brief]. National Center for Sustainable Transportation. https://doi.org/10.7922/G2FB5177

Du, H., Zhao, J., Zhao, Y., Xu, S., Lin, X., Chen, Y., Gardner, L. M., & Yang, H. F. (2024). *Advancing real-time pandemic forecasting using large language models: A COVID-19 case study* [Preprint]. arXiv. https://doi.org/10.48550/arXiv.2404.06962

Elhedhli, S., & Gzara, F. (2008). Integrated design of supply chain networks with three echelons, multiple commodities and technology selection. *IIE Transactions, 40*(1), 31–44. https://doi.org/10.1080/07408170701246641

Erlebacher, S. J., & Meller, R. D. (2000). The interaction of location and inventory in designing distribution systems. *IIE Transactions, 32*(2), 155–166. https://doi.org/10.1080/07408170008963888

Fink, A. (2020). *Conducting research literature reviews: From the Internet to paper* (5th ed.). SAGE.

Friday, D., Savage, D. A., Melnyk, S. A., Harrison, N., Ryan, S., & Wechtler, H. (2021). A collaborative approach to maintaining optimal inventory and mitigating stockout risks during a pandemic: Capabilities for enabling health-care supply chain resilience. *Journal of Humanitarian Logistics and Supply Chain Management, 11*(2), 248–271. https://doi.org/10.1108/JHLSCM-07-2020-0061

Ghafour, K. M., & Aljanabi, A. R. A. (2023). The role of forecasting in preventing supply chain disruptions during the COVID-19 pandemic: A distributor–retailer perspective. *Operations Management Research, 16*(2), 780–793. https://doi.org/10.1007/s12063-022-00327-y

Göksu, A., Kocamaz, U. E., & Uyaroğlu, Y. (2015). Synchronization and control of chaos in supply chain management. *Computers & Industrial Engineering, 86*, 107–115. https://doi.org/10.1016/j.cie.2014.09.025

Grant, M. J., & Booth, A. (2009). A typology of reviews: An analysis of 14 review types and associated methodologies. *Health Information & Libraries Journal, 26*(2), 91–108. https://doi.org/10.1111/j.1471-1842.2009.00848.x

Gružauskas, V., & Burinskienė, A. (2022). Managing supply chain complexity and sustainability: The case of the food industry. *Processes, 10*(5), Article 852. https://doi.org/10.3390/pr10050852

Gultekin, B., Demir, S., Gunduz, M. A., Cura, F., & Ozer, L. (2022). The logistics service providers during the COVID-19 pandemic: The prominence and the cause-effect structure of uncertainties and risks. *Computers & Industrial Engineering, 165*, Article 107950. https://doi.org/10.1016/j.cie.2022.107950

Gupta, S., Bag, S., Modgil, S., Lopes de Sousa Jabbour, A. B., & Kumar, A. (2022). Examining the influence of big data analytics and additive manufacturing on supply chain risk control and resilience: An empirical study. *Computers & Industrial Engineering, 172*, Article 108629. https://doi.org/10.1016/j.cie.2022.108629

Hallegatte, S. (2014). *Economic resilience: Definition and measurement* (Policy Research Working Paper No. 6852). World Bank. https://doi.org/10.1596/1813-9450-6852

Hosseini, S., Ivanov, D., & Dolgui, A. (2019). Review of quantitative methods for supply chain resilience analysis. *Transportation Research Part E: Logistics and Transportation Review, 125*, 285–307. https://doi.org/10.1016/j.tre.2019.03.001

Hsu, C.-H., He, X., Zhang, T.-Y., Chang, A.-Y., Liu, W.-L., & Lin, Z.-Q. (2022). Enhancing supply chain agility with Industry 4.0 enablers to mitigate ripple effects based on integrated QFD-MCDM: An empirical study of new energy materials manufacturers. *Mathematics, 10*(10), Article 1635. https://doi.org/10.3390/math10101635

Instituto Nacional de Estadística y Geografía. (n.d.-a). *Banco de Información Económica (BIE)*. Retrieved 1 August 2026, from https://www.inegi.org.mx/app/indicadores/?tm=0

Instituto Nacional de Estadística y Geografía. (n.d.-b). *Producto interno bruto por entidad federativa (PIBE): Año base 2018*. Retrieved 1 August 2026, from https://www.inegi.org.mx/programas/pibent/2018/

Islam, S., Shi, Y., Ahmed, J. U., & Uddin, M. J. (2019). Minimization of empty container truck trips: Insights into truck-sharing constraints. *The International Journal of Logistics Management, 30*(2), 641–662. https://doi.org/10.1108/IJLM-08-2018-0191

Ivanov, D. (2022). Lean resilience: AURA (Active Usage of Resilience Assets) framework for post-COVID-19 supply chain management. *The International Journal of Logistics Management, 33*(4), 1196–1217. https://doi.org/10.1108/IJLM-11-2020-0448

Ivanov, D., Tang, C. S., Dolgui, A., Battini, D., & Das, A. (2021). Researchers' perspectives on Industry 4.0: Multi-disciplinary analysis and opportunities for operations management. *International Journal of Production Research, 59*(7), 2055–2078. https://doi.org/10.1080/00207543.2020.1798035

Juan, S.-J., Li, E. Y., & Hung, W.-H. (2022). An integrated model of supply chain resilience and its impact on supply chain performance under disruption. *The International Journal of Logistics Management, 33*(1), 339–364. https://doi.org/10.1108/IJLM-03-2021-0174

Li, G., & Xia, Y. (2023). A supply chain sourcing model at the interface of operations and sustainability. *IISE Transactions, 55*(8), 794–806. https://doi.org/10.1080/24725854.2022.2111481

Lorenc, A., & Kuźnar, M. (2021). The most common type of disruption in the supply chain—Evaluation based on the method using artificial neural networks. *International Journal of Shipping and Transport Logistics, 13*(1/2), 1–24. https://doi.org/10.1504/IJSTL.2021.112910

Mari, S. I., Lee, Y. H., Memon, M. S., Park, Y. S., & Kim, M. (2015). Adaptivity of complex network topologies for designing resilient supply chain network. *International Journal of Industrial Engineering: Theory, Applications and Practice, 22*(1), 102–116. https://doi.org/10.23055/IJIETAP.2015.22.1.1326

Martin, R., & Sunley, P. (2015). On the notion of regional economic resilience: Conceptualization and explanation. *Journal of Economic Geography, 15*(1), 1–42. https://doi.org/10.1093/jeg/lbu015

Moses, M., & Seshadri, S. (2000). Policy mechanisms for supply chain coordination. *IIE Transactions, 32*(3), 245–262. https://doi.org/10.1023/A:1007646531546

Nagy, J., & Foltin, P. (2022). Increase supply chain resilience by applying early warning signals within big-data analysis. *Ekonomski Vjesnik, 35*(2), 467–481. https://doi.org/10.51680/ev.35.2.17

Negri, M., Cagno, E., Colicchia, C., & Sarkis, J. (2021). Integrating sustainability and resilience in the supply chain: A systematic literature review and a research agenda. *Business Strategy and the Environment, 30*(7), 2858–2886. https://doi.org/10.1002/bse.2776

Nembhard, H. B., Shi, L., & Aktan, M. (2005). A real-options-based analysis for supply chain decisions. *IIE Transactions, 37*(10), 945–956. https://doi.org/10.1080/07408170591008073

Note: This reference itself contains no Chowdhury or Moktadir author. The malformed “Md.” issue belongs to other records in the list; the submitted Islam et al. authors are valid as written.

Notteboom, T., Pallis, T., & Rodrigue, J.-P. (2021). Disruptions and resilience in global container shipping and ports: The COVID-19 pandemic versus the 2008–2009 financial crisis. *Maritime Economics & Logistics, 23*(2), 179–210. https://doi.org/10.1057/s41278-020-00180-5

Nur, F., Aboytes-Ojeda, M., Castillo-Villar, K. K., & Marufuzzaman, M. (2021). A two-stage stochastic programming model for biofuel supply chain network design with biomass quality implications. *IISE Transactions, 53*(8), 845–868. https://doi.org/10.1080/24725854.2020.1751347

Olivares-Aguila, J., & Vital-Soto, A. (2021). Supply chain resilience roadmaps for major disruptions. *Logistics, 5*(4), Article 78. https://doi.org/10.3390/logistics5040078

Organisation for Economic Co-operation and Development. (2022). *International trade during the COVID-19 pandemic: Big shifts and uncertainty*. OECD Publishing. https://doi.org/10.1787/d1131663-en

Ponomarov, S. Y., & Holcomb, M. C. (2009). Understanding the concept of supply chain resilience. *The International Journal of Logistics Management, 20*(1), 124–143. https://doi.org/10.1108/09574090910954873

Rajesh, R. (2016). Forecasting supply chain resilience performance using grey prediction. *Electronic Commerce Research and Applications, 20*, 42–58. https://doi.org/10.1016/j.elerap.2016.09.006

Rajesh, R. (2019). Social and environmental risk management in resilient supply chains: A periodical study by the Grey-Verhulst model. *International Journal of Production Research, 57*(11), 3748–3765. https://doi.org/10.1080/00207543.2019.1566656

Rajesh, R., & Rajendran, C. (2019). Grey- and rough-set-based seasonal disaster predictions: An analysis of flood data in India. *Natural Hazards, 97*(1), 395–435. https://doi.org/10.1007/s11069-019-03651-y

Rajesh, R., Ravi, V., & Venkata Rao, R. (2015). Selection of risk mitigation strategy in electronic supply chains using grey theory and digraph-matrix approaches. *International Journal of Production Research, 53*(1), 238–257. https://doi.org/10.1080/00207543.2014.948579

Ramsey, A. F., Goodwin, B. K., Hahn, W. F., & Holt, M. T. (2021). Impacts of COVID-19 and price transmission in U.S. meat markets. *Agricultural Economics, 52*(3), 441–458. https://doi.org/10.1111/agec.12628

Rose, A., & Liao, S.-Y. (2005). Modeling regional economic resilience to disasters: A computable general equilibrium analysis of water service disruptions. *Journal of Regional Science, 45*(1), 75–112. https://doi.org/10.1111/j.0022-4146.2005.00365.x

Sáinz Bernat, N., Schulte, F., Voß, S., & Böse, J. (2016). Empty container management at ports considering pollution, repair options, and street-turns. *Mathematical Problems in Engineering, 2016*, Article 3847163. https://doi.org/10.1155/2016/3847163

Salehi, A., Babaei, A., & Hamidi, H. (2026). AI-driven strategies for supply chain resilience: A review of challenges and solutions during pandemics. *International Journal of Engineering, 39*(3), 585–605. https://doi.org/10.5829/ije.2026.39.03c.03

Schreiber, T. (2000). Measuring information transfer. *Physical Review Letters, 85*(2), 461–464. https://doi.org/10.1103/PhysRevLett.85.461

Sheffi, Y. (2015). *The power of resilience: How the best companies manage the unexpected*. MIT Press. https://doi.org/10.7551/mitpress/9780262029797.001.0001

Silverman, D. (Ed.). (2021). *Qualitative research* (5th ed.). SAGE.

Tashakkori, A., & Teddlie, C. (Eds.). (2010). *SAGE handbook of mixed methods in social & behavioral research* (2nd ed.). SAGE. https://doi.org/10.4135/9781506335193

Thomas, A. V., & Mahanty, B. (2020). Interrelationship among resilience, robustness, and bullwhip effect in an inventory and order based production control system. *Kybernetes, 49*(3), 732–752. https://doi.org/10.1108/K-11-2018-0588

U.S. Bureau of Transportation Statistics. (n.d.). *Tonnage for internal U.S. waterways* [Data set]. FRED, Federal Reserve Bank of St. Louis. Retrieved 5 January 2026, from https://fred.stlouisfed.org/series/WATERBORNED11

Waller, M. A., & Fawcett, S. E. (2013). Data science, predictive analytics, and big data: A revolution that will transform supply chain design and management. *Journal of Business Logistics, 34*(2), 77–84. https://doi.org/10.1111/jbl.12010

Wang, J., Dou, R., Muddada, R. R., & Zhang, W. (2018). Management of a holistic supply chain network for proactive resilience: Theory and case study. *Computers & Industrial Engineering, 125*, 668–677. https://doi.org/10.1016/j.cie.2017.12.021

Wang, J., Swartz, C. L. E., Corbett, B., & Huang, K. (2020). Supply chain monitoring using principal component analysis. *Industrial & Engineering Chemistry Research, 59*(27), 12487–12503. https://doi.org/10.1021/acs.iecr.0c01038

Wide, P. (2020). Improving decisions support for operational disruption management in freight transport. *Research in Transportation Business & Management, 37*, Article 100540. https://doi.org/10.1016/j.rtbm.2020.100540

Yang, B., Ge, S., Liu, H., Li, J., & Zhang, S. (2022). Resilience assessment methodologies and enhancement strategies of multi-energy cyber-physical systems of the distribution network. *IET Energy Systems Integration, 4*(2), 171–191. https://doi.org/10.1049/esi2.12067

Zeng, B., & Yen, B. P.-C. (2017). Rethinking the role of partnerships in global supply chains: A risk-based perspective. *International Journal of Production Economics, 185*, 52–62. https://doi.org/10.1016/j.ijpe.2016.12.004

Zhang, Y., & Zhang, Z.-H. (2019). Impact of the cannibalization effect between new and remanufactured products on supply chain design and operations. *IISE Transactions, 51*(1), 22–40. https://doi.org/10.1080/24725854.2018.1486055

Zhao, W., & Wang, Y. (2002). Coordination of joint pricing–production decisions in a supply chain. *IIE Transactions, 34*(8), 701–715. https://doi.org/10.1023/A:1014972527002

Zhao, Y., Xue, Q., & Zhang, X. (2018). Stochastic empty container repositioning problem with CO_2 emission considerations for an intermodal transportation system. *Sustainability, 10*(11), Article 4211. https://doi.org/10.3390/su10114211

Zheng, G., Kong, L., & Brintrup, A. (2023). Federated machine learning for privacy preserving, collective supply chain risk prediction. *International Journal of Production Research, 61*(23), 8115–8132. https://doi.org/10.1080/00207543.2022.2164628

Zogaan, W. A., Ajabnoor, N., & Salamai, A. A. (2025). Leveraging deep learning for risk prediction and resilience in supply chains: Insights from critical industries. *Journal of Big Data, 12*, Article 94. https://doi.org/10.1186/s40537-025-01143-4